

The Journal of Neuroscience

<http://jneurosci.msubmit.net>

The RNA-binding protein HuR controls global changes in gene expression during Schwann cell development

JN-RM-5868-11R2

Ashwin Woodhoo, CIC Biogune

Marta Iruarrizaga-Lejarreta, CIC Biogune

Marta Varela-Rey, CIC Biogune

Juan José Lozano, CIBERehd. Hospital Clinic Centre Esther Koplovitz

David Fernández-Ramos, CIC Biogune

Naiara Rodríguez-Ezpeleta, CIC Biogune

Nieves Embade, CIC Biogune

Shelly Lu, University of Southern California

Peter Van der Kraan, Radboud University Nijmegen Medical Centre

Esmeralda Blaney Davidson, Radboud University Nijmegen Medical Centre

Myriam Gorospe, National Institutes of Health

Rhona Mirsky, University College London

Kristjan R. Jessen, University College London

ana aransay, CIC bioGUNE

José Mato, CIC Biogune Research Institute

María Martínez-Chantar, CIC Biogune Research Institute

Commercial Interest: No

Title: The RNA-binding protein HuR controls global changes in gene expression during Schwann cell development

Abbreviated Title: *HuR controls gene expression in Schwann cells*

Authors: Marta Iruarrizaga-Lejarreta¹, Marta Varela-Rey¹, Juan José Lozano², David Fernández-Ramos¹, Naiara Rodríguez-Ezpeleta¹, Nieves Embade¹, Shelly C Lu³, Peter M van der Kraan⁴, Esmeralda N Blaney Davidson⁴, Myriam Gorospe⁵, Rhona Mirsky⁶, Kristján R Jessen⁶, Ana María Aransay¹, José M Mato¹, María L Martínez-Chantar¹, Ashwin Woodhoo^{1^*}

¹CIC bioGUNE, Centro de Investigación Biomédica en Red de Enfermedades Hepáticas y Digestivas (CIBERehd), Technology Park of Bizkaia, 48160-Derio, Bizkaia, Spain.

²CIBERehd. Hospital Clinic Centre Esther Koplovitz (CEK) C/ Rosselló 153 subsuelo 08036 Barcelona; Spain

³Division of Gastrointestinal and Liver Diseases, USC Research Center for Liver Diseases, Keck School of Medicine, University of Southern California, Los Angeles, CA 90033, USA.

⁴Experimental Rheumatology & Advanced Therapeutics, Department of Rheumatology, RUNMC, Radboud University Nijmegen Medical Centre, NCMLS, Medical Centre Nijmegen, Geert Grooteplein 28, 6525 GA Nijmegen, Netherlands

⁵Laboratory of Cellular and Immunology, National Institute on Aging-Intramural Research Program, National Institutes of Health, Baltimore, Maryland, USA

⁶Department of Cell and Developmental Biology, University College London, Gower Street, London WC1E 6BT, UK.

[^] *Joint senior authors*

Corresponding Author: Ashwin Woodhoo, CIC bioGUNE, Technology Park of Bizkaia, 48160 Derio, Bizkaia, Spain. **Tel:** +34-944-061318; **Fax:** +34-944-061301. **E-mail:** awoodhoo@cicbiogune.es

Number of Pages: 48

Number of Figures: 10

Number of Tables: 1

Number of Words in Abstract: 159

Number of Words in Introduction: 500

Number of Words in Discussion: 1500

Acknowledgements: This work was supported by grants from Instituto de Salud Carlos III (FIS, PS09/00094; Ministry of Health, Spain), Fundación Científica de la Asociación Española Contra el Cáncer AECC (Cancer Infantil) and the Program Ramón y Cajal (Ministry of Science and Innovation, Spain) to AW and an International Joint Project grant from the Royal Society of Great Britain (to KRJ and AW), NIH AT-1576 (to SCL, MLMC and JMM), SAF 2008-04800 (to JMM), Sanidad Gobierno Vasco 2012 (to MVR), ETORTEK-2010 (to MLMC), Sanidad Gobierno Vasco 2008 (to MLMC), Educación Gobierno Vasco 2011 (to MLMC), PI11/01588 (to MLMC). CIBERehd is funded by the Instituto de Salud Carlos III. MG was supported by the NIA-IRP, NIH. All authors declare no conflict of interest.

ABSTRACT

An important prerequisite to myelination in peripheral nerves is the establishment of one-to-one relationships between axons and Schwann cells. This patterning event depends on immature Schwann cell proliferation, apoptosis and morphogenesis, which are governed by co-ordinated changes in gene expression. Here, we found that the RNA-binding protein HuR was highly expressed in immature Schwann cells, where genome-wide identification of its target mRNAs *in vivo* in mouse sciatic nerves using ribonomics showed an enrichment of functionally-related genes regulating these processes. HuR co-ordinately regulated expression of several genes to promote proliferation, apoptosis and morphogenesis in rat Schwann cells, in response to NRG1, TGF β and laminins, three major signals implicated in this patterning event. Strikingly, HuR also binds to several mRNAs encoding myelination-related proteins, but contrary to its typical function, negatively regulated their expression, likely to prevent ectopic myelination during development. These functions of HuR correlated with its abundance and subcellular localisation, which were regulated by different signals in Schwann cells.

INTRODUCTION

The myelinating Schwann cells in the peripheral nervous system (PNS) are derived from the neural crest via two transitional stages. First, neural crest cells generate Schwann cell precursors, which then give rise to immature Schwann cells that surround large bundles of axons. Schwann cells then initiate radial sorting of axons by selectively segregating large-diameter axons and establishing one-to-one relationships with them. This prerequisite for myelination requires the matching of Schwann cell number to axons by proliferation and apoptosis, and cytoskeletal-mediated Schwann cell morphogenesis; processes controlled by 3 major signals: Neuregulin-1 (NRG1), Transforming Growth Factor β (TGF β) and laminins (Woodhoo and Sommer, 2008; Jessen and Mirsky, 2005).

Global changes in gene expression accompany the profound phenotypic changes associated with Schwann cell development. Thus, genes associated with proliferation and apoptosis, which reach a peak in immature Schwann cells, are highly expressed at this stage. With subsequent development, as the cells exit the cell cycle and lose susceptibility to apoptosis, these genes are downregulated. Conversely, many myelination-related genes are significantly upregulated as immature Schwann cells differentiate into myelinating Schwann cells (Verheijen *et al.*, 2003; D' Antonio *et al.*, 2006b). Recent studies have started to unravel the transcriptional and post-transcriptional molecular mechanisms that control these coordinated changes in gene expression. Chromatin remodelling, via HDAC1 and HDAC2, and microRNAs have been shown to be essential for the control of Schwann cell numbers and induction of myelination (Chen *et al.*, 2011; Jacob *et al.*, 2011; Dugas and Notterpek, 2011).

Cytoplasmic control of mRNA turnover and translation rates, mediated by RNA-binding proteins (RBPs), is a major post-transcriptional mechanism that promotes rapid and appropriate spatiotemporal expression of encoded proteins in response to environmental and internal cues. Hu antigen R (HuR), a member of the ELAV/Hu family of RBPs, is a ubiquitously expressed protein that is essential for embryonic development and plays an important role in a number of disorders, including cancer (Hinman and Lu, 2008; Vazquez-Chantada *et al.*, 2009). HuR binds to the U- and AU-rich elements (ARE) in the 3' untranslated region (UTR) of many mRNAs, generally promoting their stability and translation (Mukherjee *et al.*, 2011; Lebedeva *et al.*, 2011).

In this study, we found that HuR was highly expressed in immature Schwann cells, where genome-wide identification of its target mRNAs showed an enrichment of mRNAs encoding proteins with functions in regulating proliferation, apoptosis and morphogenesis. Using *in vitro* silencing experiments, we found that HuR contributed to enhancing the expression of several genes induced by NRG1, TGF β and laminins, the 3 major signals involved in these processes. Chromatin immunoprecipitation analysis showed that p65 and SMAD 2/3 bind to the *HuR* promoter *in vivo* to regulate its expression, likely to be triggered by NRG1 and TGF β respectively. Significantly, we found that HuR is a negative regulator of myelination since, although it is bound to several mRNAs encoding myelination-related proteins, it negatively regulated their expression. Finally, we found that HuR protein is greatly reduced *in vivo* as myelination progresses, a process likely to be controlled by Egr2-mediated ubiquitin proteolysis.

MATERIALS AND METHODS

Animals

Mice and rats of either sex were housed at the Animal unit at CIC bioGUNE, and all procedures were approved by the institutional review committee on animal use. The CIC bioGUNE's Animal Unit is an AAALAC accredited facility.

RNA immunoprecipitation (IP).

IP protocol of endogenous mRNA–transfected HuR complexes was performed as described in Keene et al. (2006). In brief, 500 µg of whole-cell lysate obtained from a pool of NB or P5 sciatic nerves from C57BL6J mice of either sex were incubated with a suspension of Protein A–Sepharose beads (Sigma-Aldrich), pre-coated with 15 µg of either IgG1 (BD Pharmingen) or anti-HuR (Santa Cruz Biotechnology) antibodies. For RIP-chip analysis, appropriate amounts of total RNA from four biological replicates of HuR and Mock IPs, as well as 2 replicates of input mRNA from NB and P5 nerves were submitted to the Genomics Analysis Platform at CIC bioGUNE for analysis on MOUSE WG-6 V2 arrays (Illumina). For RIP-qPCR analysis, bound mRNA was measured by real-time PCR analysis, normalized to *GAPDH* mRNA bound in a non-specific manner to IgG1.

Microarray analysis and GO classification

Data were extracted using BeadStudio data analysis software. Data were processed and normalised using Robust Spline normalisation using Lumi bioconductor package (Du *et al.*, 2008). The data for the probes with a detection p-value higher or equal to 0.01 were excluded. Those detected with p-value lower than 0.01 in at least one

array were accepted as significant. For the detection of differentially expressed genes, a linear model was fitted to the data and empirical Bayes moderated t-statistics were calculated using the limma package from Bioconductor. Adjustment of p-values was done by the determination of false discovery rates (FDR) using Benjamini-Hochberg procedure (Smyth, 2005; Peart *et al.*, 2005). Biological functional analysis was performed using the Ingenuity Pathway Analysis software (Ingenuity Systems, Redwood City, CA). Fisher's exact test was performed with the *P* value threshold of 0.05 to identify molecular functional categories with statistical significance.

Biotin Pull-Down Assay

Biotinylated transcripts were synthesized using cDNA that was prepared from sciatic nerves. Templates were prepared using forward primers that contained the T7 RNA polymerase promoter sequence (CCAAGCTTCTAATACGACTCACTATAGGAGA), as described (Li *et al.*, 2002). Biotin pull-down assays were performed as described elsewhere (Antic and Keene, 1997) and bound proteins were analyzed by Western blotting. In brief, the PCR-amplified fragments were purified and used as templates for *in vitro* synthesis of the corresponding biotinylated RNAs by MAXIscript kit (Applied Biosystems). Biotin pull-down assays were performed by incubating 40 μ g of P5 sciatic nerve cell lysates with equimolar amounts of biotinylated transcripts for 1 hr at room temperature. The complexes were isolated using paramagnetic streptavidin-conjugated Dynabeads (Invitrogen), and bound proteins in the pull-down material were analyzed by Western blotting using an antibody recognizing HuR. Primer sequences are available on request.

RNA isolation and quantitative PCR (qPCR).

RNA was isolated with Trizol (Invitrogen) and its concentration and integrity determined. qPCRs were performed using BioRad iCycler thermocycler. Ct values were normalized to the housekeeping expression (*GAPDH*). Primer sequences are available on request.

Protein isolation and Western blotting.

Isolation and Western blotting of total proteins from cells and nerves were done as described (Parkinson *et al.*, 2008). Subcellular fractions were isolated using the Proteoextract Subcellular Proteome Extraction kit (Calbiochem), according to manufacturer's instructions. The purity of cytoplasmic and nuclear fractions was examined by Western blotting in each experiment using antibodies to Gapdh and Histone H3 respectively.

Rat primary Schwann cell culture

Sciatic nerves obtained from P3 Wistar rats of either sex were digested in 0.25% trypsin, 0.4% collagenase in DMEM, and cultured for 3 days in DMEM with 10% fetal bovine serum (FBS) containing AraC (10^{-3} M). After 3 days in culture, Schwann cells were immunopanned to remove remaining fibroblasts and expanded in DMEM/F12, 3% FBS, NRG1 (10 ng/ml), N2 supplement and Forskolin (4 μ M). Only the first 5 passages were used. For proliferation experiments, cells were first cultured overnight in Minimal Medium (MM: DMEM/F12, 5% FBS, and N2 supplement) before NRG1 (20 ng/ml) or TGF β (2 ng/ml) stimulation at appropriate time-points. For cell shape experiments, cells were cultured overnight in MM before replating onto PDL- or

laminin-coated dishes. For apoptosis assays, freshly isolated Schwann cells from NB nerves were isolated, plated onto coverslips in Simple Medium [SM: DMEM/F12 and BSA (0.3 mg/ml final)] and treated with TGF β (2 ng/ml) for 48 hrs. Recombinant human TGF β 1 and NRG-1 (Heregulin- β 1 isoform) were purchased from Peprotech and R&D Systems respectively.

Neuron-Schwann cell co-cultures

Myelinating neuron-Schwann cell co-cultures were prepared by adding purified rat Schwann cells, infected with sh HuR lentivirus or adenovirus expressing HuR, to purified E15 rat DRG neurons. Myelination was induced with 50mg/ml ascorbic acid and MBP antibodies were used to label myelin segments or RNA extracted (Parkinson *et al.*, 2008).

Viral Infection

For HuR knockdown, cells were treated with short-hairpin lentiviral particles against HuR [CCGGCCCACAAATGTTAGACCAATTCTCGAGAATTGGTCTAACATTTGTGGGTTTTTG] in the presence of hexadimethrine bromide (8 μ g/ml). After 24 hrs transduction, the cells were selected using puromycin (1.25 μ g/ml) and puromycin-resistant HuR-knockdown cell clones were grown, analyzed, and frozen for future use. For adenoviral infections, cells were cultured in MM, adenoviral particles added (amount added determined by titration) and 24 hrs later the medium changed. Adenoviral constructs used were: GFP/Krox-20 (Ad-K20) and its matched GFP control (Ad-GFP), a gift from J. Milbrandt (Parkinson *et al.*, 2004); SMAD7 (Ad-SMAD7) (Blaney-Davidson *et al.*, 2006) and HuR (Ad-HuR) (Xiao *et al.*, 2007).

Inhibitors

Specific inhibitors in our culture experiments were obtained from Calbiochem and were used at the following concentrations: 10 μ M UO126 (Erk 1/2 inhibitor), 10 μ M SB203580 (p38 inhibitor), 10 μ M LY294002 (PI3K inhibitor), 10 μ M MG132 (Proteasome inhibitor) and 2 μ M BAY11-7082 (NF κ B inhibitor).

Migration assay

Migration using the “scratch-assay” was performed as described previously (Liang *et al.*, 2007). In brief, control and *HuR*-silenced cells were seeded onto PDL- or laminin-coated dishes and cultured overnight in MM. A scratch was performed using a p200 pipette tip, cultured medium changed and pictures taken at time 0, 6, 12, 18 and 24 hrs. The gap distance was measured at each time-point and data expressed as percentage gap distance over time.

***cAMP* myelination assay**

A cAMP analogue, dibutyl cAMP (Sigma, UK) was added to cultures (10^{-3} M), and protein or mRNA obtained 24 hrs later.

Immunohistochemistry (IHC) and immunocytochemistry (ICC).

For teased nerves, nerves were dissected out, immediately fixed in 4% PFA for 10 min, teased on microscope slides and allowed to dry. The samples were incubated in 0.2% triton in blocking solution (BS: PBS containing 10% calf serum, 0.1% lysine and 0.02 % sodium azide) followed by overnight incubation at 4⁰C with the following primary antibodies: HuR (1:100) and TUJ1 (1:5000) followed by secondary

antibodies conjugated with FITC or Cy3 (Cappel/Jackson Immunoresearch Labs). Talin ICC has been described elsewhere (Nodari *et al.*, 2007), and *in vitro* BrdU incorporation and TUNEL labeling described elsewhere (D' Antonio *et al.*, 2006a; Parkinson *et al.*, 2001). Images were acquired with an AxioImager D1 fluorescent microscope (Zeiss).

Chromatin Immunoprecipitation (ChIP)

Rat Schwann cells or whole nerves were cross-linked with 1% formaldehyde (vol/vol) at 25 °C for 10 min. After sonication into 200–500-bp fragments using Bioruptor (Diagenode), chromatin was immunoprecipitated with 2 µg of anti-p65 antibody (sc-372, Santa Cruz Biotechnology) or 5 µg of anti-Smad2/3 antibody (3102, Cell Signaling Technology) using the Magna ChIP G kit (Millipore). The recovered DNA was subjected to PCR amplification. Chromatin that was immunoprecipitated with mouse IgG was used as a negative control. The abundance of target genome DNA was calculated as the percentage of input. Primer sequences are available on request.

Antibodies

Antibodies used were from: HuR and p65 (Santa Cruz Biotechnology), Gapdh (abcam), β -actin and Talin (Sigma), p-ERK1/2, p-AKT, p-p38, Smad 2/3 (Cell Signalling Technology), Egr2 and TuJ1 (Covance), MPZ (Astexx), Periaxin (gift from P. Brophy), MBP (Eurogentec). Fluorescent-conjugated secondary antibodies were from Jackson Immunoresearch and HRP-conjugated secondary antibodies were from Biorad.

Assessment of mRNA stability

mRNA stability was determined by actinomycin D chase experiments, following a standard protocol described elsewhere (Chang *et al.*, 2010). Briefly, control and *HuR*-silenced cells were treated with db cAMP for 24 hrs, which significantly increased expression of all mRNAs analysed. Actinomycin D was added to a final concentration of 5 µg/ml to block further transcription. At 0, 30, 60, 120 and 240 min after actinomycin D treatment, the cells were harvested and mRNA was quantified by qPCR. The mRNA decay was recorded as the percentage of mRNA remaining over time compared with the amount before the addition of actinomycin D.

Statistical analysis

All data are presented as arithmetic mean \pm standard error of the mean (SEM) unless otherwise stated. Statistical significance was estimated by the Student's t-test.

RESULTS

HuR is highly expressed in immature Schwann cells

HuR is a ubiquitously expressed RBP that binds to and regulates expression of thousands of mRNAs (Mukherjee *et al.*, 2011; Lebedeva *et al.*, 2011), playing fundamental roles in proliferation, apoptosis and differentiation in several systems and cell types (Hinman and Lu, 2008). To investigate whether HuR might have a role in Schwann cell development, we first examined its expression in rat sciatic nerves at different ages, as immature Schwann cells differentiate into myelinating Schwann cells (Woodhoo *et al.*, 2009).

We found that *HuR* mRNA was highly expressed in newborn nerves (NB), which contain mostly immature Schwann cells, and post-natal day 5 (P5), which contain a mixture of immature Schwann cell and actively myelinating Schwann cells. There was a small but significant down-regulation in P10 nerves, which contain an enriched population of actively myelinating Schwann cells (Fig. 1a). This was confirmed by examining its expression in total protein extracts (Fig. 1b), although the decrease at protein level seen at P10 (about 70% by densitometry analysis) was much more significant than at mRNA level (about 25%). A similar pattern of expression was found when nuclear and cytoplasmic protein subcellular fractions were analysed (Fig. 1c). We confirmed that HuR was expressed in Schwann cells by immunohistochemistry in P5 teased nerves (Fig. 1d).

Our results indicate that HuR may have a functional role in early postnatal nerves since its abundance and cytoplasmic export both critically control expression of its target genes (Hinman and Lu, 2008).

RIP-chip identifies several HuR target genes

To examine the biological significance of the high levels of HuR in NB and P5 Schwann cells, we analysed the mRNAs bound to it on a genome-wide scale. For this, immunoprecipitation (IP) of ribonucleotide complexes (RNPs) from cytoplasmic lysates of freshly isolated NB and P5 mouse sciatic nerves using an affinity-purified HuR antibody was carried out, followed by purification and genome-wide micro-array analysis of bound mRNAs (RIP-chip).

Two populations of mRNAs were detected in our analysis: an enriched population corresponding to the HuR-bound mRNAs and a non-enriched population representing background (control IP using mouse IgG) (Fig. 2a). To identify transcripts significantly associated with HuR, we used median log ratios of signal from RNA immunoprecipitation with HuR antibody versus the control IgG. HuR bound to 275 and 90 transcripts in NB and P5 nerves respectively (Fig. 2b,c)

Next we examined the relationship between the levels of each HuR-bound transcript relative to its total cellular level. There was little correlation between the probability of HuR association and the transcriptome, with only about 25 % of total identified transcripts (HuR IP/IgG IP), found to be significantly enriched relative to total mRNA levels (HuR IP/Input), in both cases (Fig. 2b). This shows that detection of transcripts in HuR IP fraction is not dependent on mRNA abundance and that there is no bias towards identification of highly abundant or transcribed genes, as shown in other systems (Mukherjee *et al.*, 2009; Hieronymus and Silver, 2003).

Comparison of the identified transcripts in the NB and P5 nerves showed that about two thirds of targets identified in P5 nerves were commonly present in NB nerves, whereas the large majority of transcripts identified in NB nerves were

uniquely expressed (Fig. 2c). Using the data set of gene expression profiling in nerves of mice at different ages across the Schwann cell lineage (Verheijen *et al.*, 2003), we found that about 25% of these unique HuR targets in NB nerves were also significantly downregulated in older nerves compared to NB nerves (50 out of 215).

Since it was proposed that RBPs coordinate the expression of transcripts encoding biologically related proteins (Keene, 2007), we performed Gene Ontology (GO) analyses of differentially regulated HuR mRNA targets in NB and P5 nerves. Functional classification into Molecular and Cellular Function (MF) showed that most of the enriched genes fell into several categories related to proliferation, apoptosis and morphogenesis (Fig. 2d).

To validate our results from the RIP-chip analysis, fresh IP were carried out and expression of several genes related to proliferation, apoptosis and morphogenesis was quantified by quantitative RT-PCR (RIP-qPCR). We found that with some rare exceptions, there was a similar trend of enrichment of these HuR targets using both analyses (Table 1). Our RIP-chip analysis also revealed a significant enrichment of mRNAs encoding RBPs, including *HuR* itself, and *Thoc4* and *Hnrpl* amongst others, in line with other studies (Pullmann *et al.*, 2007; Mansfield and Keene, 2009). This was confirmed by RIP-qPCR for selected genes (data not shown).

In summary, we find that HuR is bound to several mRNA targets in peripheral nerves *in vivo*, with decreasing binding affinity as development proceeds. The identified targets generally fall into categories that most closely characterise the immature Schwann cell stage, i.e. proliferation, apoptosis and

motility/morphogenesis, suggesting that HuR may have a functional role in regulating these processes.

HuR mediates laminin-induced motility and morphogenesis

As mentioned above, prior to myelination, immature Schwann cells migrate extensively along axons and send processes within axon families to segregate and ensheath them. Laminin, one of the critical components of the basal lamina, plays a fundamental role in this process (Chernousov *et al.*, 2008; Feltri *et al.*, 2008).

To examine if HuR mediated laminin-induced function in Schwann cells, we used a lentiviral vector to silence *HuR* (see Figure 7b for effectiveness of *HuR* knockdown) and examined its effect on migration and morphogenesis. Using the cell scratch assay, we found that the migratory rate on laminin substrate was reduced in *HuR*-silenced cells compared to control cells (Fig. 3a,b), whereas no such effect was seen on Poly-L-Lysine (PDL) substrate, which promotes non-receptor-specific cell adhesion (data not shown). Similarly, on laminin substrate but not on PDL, *HuR*-silenced cells spread less and elaborated fewer lamellipodia than control cells (Fig. 3c,d). The length of axial lamellipodia on laminin substrate, which favours directional cell migration (Pankov *et al.*, 2005), was reduced after *HuR* silencing (Fig. 3e), likely causing the defects in migratory rates seen above. In addition, we found that there was reduction in number of radial lamellipodia (Fig. 3e), which are important for the insertion of processes within axons during radial sorting (Nodari *et al.*, 2007). These results show that HuR is an important mediator of laminin-induced function in Schwann cells.

Next, we investigated the mechanisms involved in these processes. First, by qPCR, we examined the expression of several of the validated HuR targets, associated with cell movement and morphogenesis in Schwann cells or in other systems, including *Pfn1* (Witke, 2004), *Marcks* (Larsson, 2006), *Igfbp5* (Yano *et al.*, 1999), *Ncam1* (Yu *et al.*, 2009), *Actin* (Chernousov *et al.*, 2008), *Ahnak* (Salim *et al.*, 2009), *Lamc1* (Chen and Strickland, 2003) and *Calm3* (Larsson, 2006). We found that culture on laminin substrate, compared to PDL, upregulated expression of several of these HuR targets (Fig. 3f). *Ahnak*, *Lamc1* and *Calm3* were not regulated by laminin (data not shown). Using RIP-qPCR analyses, we also found that culture on laminin substrate significantly increased binding of HuR to only the regulated mRNAs (Fig. 3g) and that *HuR* silencing reduced their expression (Fig. 3h), likely explaining the defects in laminin function.

HuR-mediated stabilization and translational upregulation of target mRNAs are closely linked to its subcellular localisation. It is predominantly (>90%) localized in the nucleus, but in response to different stimuli, is exported to the cytoplasm, a process modulated by several post-translational modifications, which also affects its binding to target mRNAs (Doller *et al.*, 2008). We found that laminin increased the nucleo-cytoplasmic translocation of HuR (Fig. 4a), an effect controlled by p38 phosphorylation (Fig. 4b), which has previously been shown to be important for laminin-induced cell shape changes (Berti *et al.*, 2011; Fragoso *et al.*, 2003). Treatment with the p38 inhibitor also significantly reduced Schwann cell migration on laminin substrate (Fig. 4c).

In summary, we show that laminin induces translocation of HuR from the nucleus to the cytoplasm and increases HuR-mediated stabilization of several mRNAs that regulate cell motility and morphogenesis in Schwann cells.

HuR mediates NRG1- and TGF β -induced proliferation

Immature Schwann cell proliferate vigorously during late embryonic to perinatal stages (Stewart *et al.*, 1993), a process thought to be critical for radial sorting and dependent on axonally-derived mitogens, including NRG1 and TGF β (Chernousov *et al.*, 2008; Feltri *et al.*, 2008, Woodhoo and Sommer, 2008).

Using established cell culture conditions that promote the mitogenic effect of NRG1 and TGF β *in vitro* (Atanasoski *et al.*, 2004), we found that *HuR* silencing significantly reduced proliferation induced by these two growth factors (Fig. 5a,b). The percentage of BrdU⁺ cells was significantly reduced from $77.6 \pm 2.7\%$ in control cells to $44.6 \pm 2.5\%$ in *HuR*-silenced cells after NRG1 treatment, and from $30.1 \pm 1.5\%$ to $17.8 \pm 1.1\%$ after TGF β treatment ($p < 0.01$). To investigate the mechanisms involved in this function of HuR, we first examined expression of HuR targets associated with proliferation, including *Cyclin D1* (Kim *et al.*, 2000), *Cyclin D2* (Jena *et al.*, 2002), *Cdk2* (Tikoo *et al.*, 2000), *Serpine 2* (Lino *et al.*, 2007), *Shc1* (Ward *et al.*, 1999), *Sox9* (Lincoln *et al.*, 2007), *ErbB2* (Raphael *et al.*, 2011), *Brd4* (Houzelstein *et al.*, 2002). We found that NRG1 and TGF β treatment upregulated expression of several of these targets (Fig. 5c). RIP-qPCR analysis showed that NRG1 and TGF β treatment significantly increased HuR binding to these mRNAs (Fig. 5d), the expression of which were significantly reduced by *HuR* silencing (Fig. 5e,f). We also found that NRG1 and TGF β promoted the nucleo-cytoplasmic

translocation of HuR (Fig. 6a). ERK 1/2 and AKT phosphorylation controlled both NRG1-induced translocation of HuR and proliferation (Fig. 6b) whereas ERK 1/2 and p38 phosphorylation controlled TGF β -induced translocation of HuR and proliferation (Fig. 6c).

In summary, we show that HuR increases stability of genes in response to NRG1 and TGF β , regulating their function on proliferation.

HuR mediates TGF β -induced apoptosis

Natural cell death, like proliferation, is a feature of immature Schwann cells, which is induced by TGF β *in vivo* (D'Antonio *et al.*, 2006a).

Using established cell culture conditions that promote the apoptotic effect of TGF β in Schwann cells (Parkinson *et al.*, 2001), we found that silencing of HuR significantly reduced apoptosis (Fig. 7a,b). The percentage of surviving cells increased from 29.5 ± 8.5 % in control cells to 68.5 ± 7.8 % in *HuR*-silenced cells, whereas the percentage of apoptotic TUNEL⁺ cells decreased from 49.2 ± 6.7 % to 13.5 ± 2.3 % ($p < 0.01$). Of note, these culture conditions are different from proliferation-inducing conditions (above). To investigate the mechanisms involved, we first examined expression of HuR targets associated with apoptosis, including *Aatf* (Tomomura *et al.*, 2001), *Btg1* (Lee *et al.*, 2003), *Caspase 2* (Kumar, 2009), *Caspase 9* (Riedl and Salvesen, 2007), *Vdac1* (Shoshan-Barmatz *et al.*, 2010), *Pdcd4* (Lankat-Buttgereit and Göke, 2009), *Map3k1* (Parkinson *et al.*, 2004), *Cd44* (Rouschop *et al.*, 2006). We found that TGF β treatment upregulated expression of several of these HuR targets (Fig. 7c). RIP-qPCR analysis showed that TGF β treatment significantly increased HuR binding to them (Fig. 7d), the expression of

which was significantly reduced by *HuR* silencing (Fig. 7e). We also found that TGF β induced the nucleo-cytoplasmic translocation of HuR (Fig. 7f), an effect controlled by p38 phosphorylation but not by ERK 1/2 phosphorylation, which was not activated in these culture conditions (Fig. 7g). Treatment with specific inhibitors also had a similar effect on TGF β -induced apoptosis (Fig. 7h).

Thus, we show that TGF β -induced apoptosis is controlled by HuR-mediated stabilization of several apoptosis-related gene.

HuR is a negative regulator of myelination

In our RIP-chip analysis, we found several myelination related proteins (e.g. Pmp22, Mpz) encoded by mRNAs whose abundance was enriched in HuR IP samples, especially at the NB stage (Fig. 2b). We confirmed this observation for the *Pmp22* gene by RIP-qPCR (Fig. 8a) and showed that HuR specifically bound to its 3' UTR by biotin pull-down assays (Fig. 8b). By RIP-qPCR, we also validated the binding of HuR to other myelination-related mRNAs (i.e. *Egr2*, *Prx*, *Mbp*, *Mpz*) with significantly decreased binding affinity in P5 nerves (Fig. 8c). This was a surprising observation since this pattern is inversely correlated to their total mRNA levels, which increase postnatally reaching a peak at about P10 (Verheijen *et al.*, 2003).

To further examine the role of HuR in the process of myelination, we silenced *HuR* in cultured Schwann cells and examined expression of some of these myelination-related proteins by Western blotting. *HuR* silencing induced a significant increase in their levels, both under myelinogenic conditions and strikingly under basal conditions as well (Fig. 8d). By qPCR analysis, we also found increased levels of myelination-related mRNAs after *HuR* silencing both under basal (Fig. 8e) and

myelinogenic conditions (Fig. 8f), which was opposite to its effects seen above for morphogenesis-, proliferation- and apoptotic-related genes. Exposure to actinomycin D in cAMP-treated cells showed that the half-life of each mRNA was significantly longer in *HuR*-silenced cells than control cells (Fig. 8g) suggesting that HuR could be destabilizing these mRNAs, instead of its typical role as a stabilizing factor for target mRNAs.

These data indicate that HuR could be a negative regulator of myelination (Jessen and Mirsky, 2008). To show this, we examined myelination in Dorsal Root ganglion (DRG) co-cultures, seeded with Schwann cells with altered levels of HuR. We found that *HuR* silencing significantly increased the number of Myelin Basic Protein (MBP)⁺ segments in the co-cultures (16.5 ± 2.1 % in *HuR*-silenced cells compared to 8.1 ± 1.6 % in control cells, $p < 0.01$) (Fig. 9a), accompanied by a significant increase in transcript expression (Fig. 9b). Conversely, enforced expression of HuR by adenoviral vectors decreased the number of MBP⁺ segments (5.9 ± 0.6 % in control cells compared to 4.3 ± 0.4 % in HuR-overexpressing cells, $p < 0.05$) (Fig. 9c), accompanied by a small but significant decrease in the expression of some of these transcripts (Fig. 9d).

The above data argue for a potential role of HuR in inhibiting myelination, similar to Notch and c-Jun (Woodhoo *et al.*, 2009; Parkinson *et al.*, 2008).

***HuR* transcription is regulated by p65 and Smad 2/3**

HuR abundance plays a critical role in its function (Hinman and Lou, 2008). We showed that *HuR* mRNA levels decrease with development (Fig. 1a) and we wanted to examine the mechanisms that control this.

It has previously been shown in other systems that *HuR* transcription is positively regulated by the transcription factors (TFs) NF- κ B (Kang *et al.*, 2008) and Smads (Jeyaraj *et al.*, 2010). We tested the recruitment of NF- κ B to the *HuR* promoter in chromatin extracts from NB, P5 and P10 nerves by ChIP using antibodies against the p65 subunit of NF- κ B followed by qRT-PCR. We found significant binding of p65 to different putative consensus sites, with reduced affinity in P10 nerves compared to NB or P5 nerves (Fig. 10a). ChIP of Smad 2/3 showed similar results (Fig. 10b), whereas no recruitment was seen with ChIP of Smad 4 (data not shown). The decreased binding of p65 or Smad 2/3 to the *HuR* promoter in P10 nerves is likely due to reduced nuclear expression of these TFs in these nerves (Fig. 10c).

Next, we examined the signalling pathways that could potentially regulate this mechanism. It was previously shown that NRG1 is sufficient to activate NF- κ B in Schwann cells (Limpert and Carter, 2010). We thus tested if NRG1 was responsible for p65-mediated *HuR* transcription. We found that NRG1 treatment induced a transient increase in *HuR* mRNA and protein levels (Fig. 10d) and ChIP experiments showed that p65 was recruited to the *HuR* promoter after treatment with NRG1 for 1 hr, but not for 12 hrs (Fig. 10e), following the kinetics of NRG1-induced *HuR* transcription (Fig. 10d). NRG1-induced increase in *HuR* levels was significantly attenuated by treatment with the NF- κ B specific inhibitor BAY11-7082, which prevents nuclear localisation of p65 (Fig. 10f), confirming the role of NF- κ B in NRG1-induced *HuR* transcription.

Similarly, we found that TGF β , which induces nuclear translocation of Smad2/3 in Schwann cells (D' Antonio *et al.*, 2006a), increased *HuR* mRNA and

protein levels (Fig. 10g) and ChIP of Smad2/3 showed its recruitment to the *HuR* promoter after treatment for 1 hr, but not 12 hrs later (Fig. 10h), following the kinetics of NRG1-induced *HuR* transcription (Fig. 10g). TGF β -induced increase in HuR levels was significantly attenuated by enforced expression of Smad7 by adenoviral infection (Ad-Smad7), which prevents phosphorylation of Smad2/3 and its subsequent activation and translocation (Fig. 10i), confirming the role of Smad2/3 in TGF β -induced *HuR* transcription. Combined treatment of NRG1 and TGF β did not lead to an enhanced upregulation of HuR levels seen by separate treatments of these growth factors at 2 hrs (Figure 10j) and at 4 hrs (data not shown). Laminin treatment also had no effect on HuR transcription (data not shown).

Our data show that *HuR* transcription is dependent on the TFs NF- κ B and Smad2/3 *in vivo*, likely to be regulated by NRG1 and TGF β respectively. Reduced expression of these TFs results in decreased *HuR* mRNA levels during development.

Egr2 (Krox20) induces proteosomal degradation of HuR

Earlier we found that HuR protein levels were significantly reduced in P10 nerves compared to NB or P5 nerves, whereas there was only a slight reduction in mRNA levels (Fig. 1a-c). Since we found previously that the TF Egr2, which plays a critical role in the myelination process (Topilko *et al.*, 2004), can also suppress expression of several negative regulators of myelination, including Notch and c-Jun (Woodhoo *et al.*, 2009; Parkinson *et al.*, 2008), we examined whether it was responsible for this down-regulation of HuR expression. We found that enforced Egr2 expression was sufficient to suppress HuR protein levels (Fig. 10k) without affecting mRNA levels (data not shown). This effect was dependent on the ubiquitin-

proteosomal degradation pathway since treatment with the proteasome inhibitor MG132 diminished this effect (Fig. 10/).

DISCUSSION

Radial sorting plays a critical role in PNS myelination. We show that the RNA-binding protein HuR is highly expressed during this stage, where it is bound to and regulates expression of numerous genes regulating proliferation, apoptosis and morphogenesis. This supports the view that RBPs such as HuR perform their overall biological functions by co-ordinately regulating expression of multiple functionally-related mRNAs, known as “RNA operons” (Keene, 2007). This association of HuR with mRNAs is dynamic, with a significant decrease in the population of target mRNAs in P5 nerves compared to NB nerves, coinciding with a general decrease in mRNA expression of some of them (Verheijen *et al.*, 2003). This is in line with other studies, which show dynamic changes in the association of HuR with target mRNAs (Mazan-Mamczarz *et al.*, 2008; Mukherjee *et al.*, 2009) and supports the view that RNA accessibility partially determines the formation of RBP-mRNA complexes (Kazan *et al.*, 2010).

Schwann cell morphogenesis

Laminins play a major role in radial sorting with severe defects seen after *in vivo* ablation of laminin isoforms, receptors and downstream signalling pathways (Chernousov *et al.*, 2008; Feltri *et al.*, 2008). Our data suggest that HuR could be an important mediator of laminin-induced function in Schwann cells by binding to and stabilizing laminin-induced mRNAs. *HuR* silencing *in vitro* results in decreased migration and significantly leads to morphological phenotypes, similar to cells lacking the laminin receptor β 1-integrin or its downstream effector Rac1 (Benninger *et al.*, 2007; Nodari *et al.*, 2007). This effect is likely controlled by p38-mediated nucleo-

cytoplasmic translocation of HuR, which is an important determinant of its function (Doller *et al.*, 2008).

Schwann cell proliferation

Schwann cell proliferation is critical for matching axon and Schwann cell numbers during radial sorting, a process dependent on axonally-derived mitogens, (Chernousov *et al.*, 2008; Feltri *et al.*, 2008, Woodhoo and Sommer, 2008). NRG1 is likely to play a major role, as shown *in vitro* (Morrissey *et al.*, 1995) and *in vivo* in zebrafish (Lyons *et al.*, 2005; Raphael *et al.*, 2011). Indirect evidence also exists in mice models *in vivo*, as shown mutants lacking the downstream effector of NRG1 signaling, Cdc42 (Benninger *et al.*, 2007) and in mice with neuronal overexpression of NRG1 (Gomez-Sanchez *et al.*, 2009). TGF β is another important Schwann cell mitogen, both *in vitro* (Atanasoski *et al.*, 2004) and *in vivo* (D'Antonio *et al.*, 2006a). We show that NRG1 and TGF β increase expression and binding of HuR to several proliferation-associated genes. *HuR* silencing decreases expression of these genes and consequently proliferation. Both signals induce nucleo-cytoplasmic translocation of HuR, an effect mediated by several kinases such as ERK 1/2, which also regulate proliferation, in line with other studies for NRG1 (Echave *et al.*, 2009; Maurel and Salzer, 2000) and TGF β (Xie *et al.*, 2007). This suggests that these kinases could regulate proliferation induced by these two growth factors, by increased nucleo-cytoplasmic translocation of HuR and stabilization of critical target genes.

Schwann cell apoptosis

TGF β is also a death signal for Schwann cells (D'Antonio *et al.*, 2006a). We show that it increases expression and binding of HuR to several apoptosis-associated genes. *HuR* silencing decreases expression of these genes and consequently apoptosis. This effect is likely mediated by an increased nucleocytoplasmic translocation of HuR, induced by TGF β -mediated p38 phosphorylation, an important determinant of its function on apoptosis, as shown here and in other systems (e.g. Liao *et al.*, 2001). It is quite striking that HuR mediates the effects of one single factor in two such distinct processes as proliferation and apoptosis. It has been proposed that TGF β acts as a mitogen for cells in close contact with axons and an apoptotic signal for cells that have lost contact with axons (D' Antonio *et al.*, 2006a). Such a context could explain the dual role of HuR; TGF β , in concert with other mitogens such as NRG1 and laminins, would induce ERK1/2-mediated cytoplasmic localisation of HuR and/or increase binding to and stability of proliferation-associated genes. Upon loss of axonal contact, TGF β , alone or in concert with other death signals, would induce p38-mediated cytoplasmic localisation of HuR and/or increase binding to and stability of apoptosis-associated genes.

Negative Regulator of Myelination

Our RIP-chip analysis identified a number of myelination-related genes as HuR targets (e.g. *Egr2*, *Pmp22*, *Mpz*) in NB nerves, which was surprising since these genes are upregulated later in development. Further analysis suggests that HuR, in contrast to its typical function, decreases their stability and translation. This is in agreement with recent reports, which also show that HuR can destabilize target

mRNAs such as *p16(INK4)* and *Daf* (Chang *et al.*, 2010; Gray *et al.*, 2010) and repress translation of genes such as *p27* (Hinman and Lou, 2008). This function of HuR is likely to prevent ectopic expression of myelin genes in immature Schwann cells before they segregate into 1:1 relationship with axons, such that myelin is not abnormally formed around axon-Schwann cell families. With subsequent development, as most of the pro-myelin Schwann cells are formed, HuR no longer binds to and destabilizes these genes as shown by RIP-chip analysis of P5 nerves, allowing myelination to proceed normally.

The mechanisms that lead to this switch in binding affinity of HuR to these mRNAs at different stages of development could be regulated by different post-translational modifications (Doller *et al.*, 2008). Thus, in NB nerves, a specific post-translational modification of HuR (e.g. phosphorylation) could make it amenable to binding to these mRNAs. After radial sorting, either loss of this modification and/or a different modification, in response to myelination signals, could prevent its binding to these mRNAs. In addition, HuR abundance, which also determines its function (Hinman and Lou, 2008), could be another important factor in regulating this switch. In P10 nerves, which correspond to stages of peak of myelination, HuR levels are considerably decreased. Thus, the low levels of HuR could also explain its decreased binding to the myelin protein-related mRNAs.

Control of HuR expression

Finally, we show that the TFs NF- κ B and Smad2/3 are bound to specific sites in the *HuR* promoter *in vivo*, as shown in other systems (Kang *et al.*, 2008; Jeyaraj *et al.*, 2010). The decreased expression of *HuR* mRNA levels in P10 nerves is likely

due to a reduced activation of these TFs, as shown previously for NF- κ B (Nickols *et al.*, 2003), resulting in a decreased binding to the *HuR* promoter. We also identify NRG1 and TGF β as the signals that respectively recruit NF- κ B and Smad2/3 to the *HuR* promoter. This is likely to be important *in vivo* to maintain high levels of HuR in early postnatal nerves.

In addition, HuR has been found to auto-regulate its levels by binding to *HuR* mRNA, stabilizing it (Al-Ahmadi *et al.*, 2009) and enhancing its cytoplasmic export (Yi *et al.*, 2010). In our RIP-chip assay, we found an enrichment of *HuR* mRNA in both NB and P5 nerves, showing that HuR is likely to be regulating its stability during Schwann cell development. We also found a significant reduction of HuR protein in P10 nerves, which is unlikely to be due to the small decrease in *HuR* mRNA levels. We show instead that this could depend on ubiquitin-proteosomal degradation, as described previously (Abdelmohsen *et al.*, 2009), mediated by the transcription factor Egr2, which similarly represses expression of other negative regulators of myelination, including Notch (Woodhoo *et al.*, 2009), and c-Jun and Sox2 (Parkinson *et al.*, 2008). miRNAs could also potentially play a significant role in this process since *HuR* translation can be blocked by 2 different miRNAs, miR-519 (Abdelmohsen *et al.*, 2008) and miR-125a (Guo *et al.*, 2009) and miRNAs play a significant role in radial sorting, proliferation and apoptosis during early postnatal Schwann cell development (Dugas and Notterpek, 2011).

***In vivo* functions of HuR?**

It would be important to examine HuR function *in vivo*. Since *HuR* knockout mice are embryonically lethal (Katsanou *et al.*, 2009), Schwann cell-specific ablation

of HuR would need to be carried out using established cre mouse lines (Woodhoo *et al.*, 2009). These mice could be characterised by peripheral nerve defects, including impairment in radial sorting and/or premature myelination, given the range of features, such as laminin-induced morphological functions that HuR controls in immature Schwann cells *in vitro*. This would be similar to mice lacking different laminin isoforms, laminin receptors and downstream targets such as Rac1 (Chernousov *et al.*, 2008; Feltri *et al.*, 2008). These pleiotropic functions of HuR and the range of mRNAs it interacts with, also raise the possibility that it could have important functions in adult nerves, controlling features such as de-differentiation. Following nerve injury, for example, Schwann cells de-differentiate to a phenotype closely resembling immature Schwann cells (Jessen and Mirsky, 2008). They downregulate myelination genes, breakdown their myelin, proliferate rapidly and some of the supernumerary ones undergo apoptosis (Yang *et al.*, 2008). HuR could be mediating injury-induced responses of Schwann cells, including proliferation and apoptosis, as some of the identified HuR targets in Schwann cells such as *Cyclin D1* are re-expressed upon injury and have important physiological functions during the de-differentiation process (Kim *et al.*, 2000; Atanasoski *et al.*, 2001).

REFERENCES

- Abdelmohsen K, Srikantan S, Kuwano Y, Gorospe M (2008) miR-519 reduces cell proliferation by lowering RNA-binding protein HuR levels. *Proc Natl Acad Sci U S A* 105:20297-20302.
- Abdelmohsen K, Srikantan S, Yang X, Lal A, Kim HH, Kuwano Y, Galban S, Becker KG, Kamara D, de Cabo R, Gorospe M (2009) Ubiquitin-mediated proteolysis of HuR by heat shock. *Embo J* 28:1271-1282.
- Al-Ahmadi W, Al-Ghamdi M, Al-Haj L, Al-Saif M, Khabar KS (2009) Alternative polyadenylation variants of the RNA binding protein, HuR: abundance, role of AU-rich elements and auto-Regulation. *Nucleic Acids Res* 37:3612-3624.
- Antic D, Keene JD (1997) Embryonic lethal abnormal visual RNA-binding proteins involved in growth, differentiation, and posttranscriptional gene expression. *Am J Hum Genet* 61:273-278.
- Atanasoski S, Notterpek L, Lee HY, Castagner F, Young P, Ehrenguber MU, Meijer D, Sommer L, Stavnezer E, Colmenares C, Suter U (2004) The protooncogene *Ski* controls Schwann cell proliferation and myelination. *Neuron* 43:499-511.
- Atanasoski S, Shumas S, Dickson C, Scherer SS, Suter U (2001) Differential cyclin D1 requirements of proliferating Schwann cells during development and after injury. *Mol Cell Neurosci* 18:581-592.
- Benninger Y, Thurnherr T, Pereira JA, Krause S, Wu X, Chrostek-Grashoff A, Herzog D, Nave KA, Franklin RJ, Meijer D, Brakebusch C, Suter U, Relvas JB (2007) Essential and distinct roles for *cdc42* and *rac1* in the regulation of Schwann cell biology during peripheral nervous system development. *J Cell Biol* 177:1051-1061.
- Berti C, Bartesaghi L, Ghidinelli M, Zambroni D, Figlia G, Chen ZL, Quattrini A, Wrabetz L,

- Feltri ML (2011) Non-redundant function of dystroglycan and beta1 integrins in radial sorting of axons. *Development* 138:4025-4037.
- Blaney Davidson EN, Vitters EL, van den Berg WB, van der Kraan PM (2006) TGF beta-induced cartilage repair is maintained but fibrosis is blocked in the presence of Smad7. *Arthritis Res Ther* 8:R65.
- Chang N, Yi J, Guo G, Liu X, Shang Y, Tong T, Cui Q, Zhan M, Gorospe M, Wang W (2010) HuR uses AUF1 as a cofactor to promote p16INK4 mRNA decay. *Mol Cell Biol* 30:3875-3886.
- Chen Y, Wang H, Yoon SO, Xu X, Hottiger MO, Svaren J, Nave KA, Kim HA, Olson EN, Lu QR (2011) HDAC-mediated deacetylation of NF-kappaB is critical for Schwann cell myelination. *Nat Neurosci* 14:437-441.
- Chen ZL, Strickland S (2003) Laminin gamma1 is critical for Schwann cell differentiation, axon myelination, and regeneration in the peripheral nerve. *J Cell Biol* 163:889-899.
- Chernousov MA, Yu WM, Chen ZL, Carey DJ, Strickland S (2008) Regulation of Schwann cell function by the extracellular matrix. *Glia* 56:1498-1507.
- D'Antonio M, Droggiti A, Feltri ML, Roes J, Wrabetz L, Mirsky R, Jessen KR (2006) TGFbeta type II receptor signaling controls Schwann cell death and proliferation in developing nerves. *J Neurosci* 26:8417-8427.
- D'Antonio M, Michalovich D, Paterson M, Droggiti A, Woodhoo A, Mirsky R, Jessen KR (2006) Gene profiling and bioinformatic analysis of Schwann cell embryonic development and myelination. *Glia* 53:501-515.
- Doller A, Pfeilschifter J, Eberhardt W (2008) Signalling pathways regulating nucleocytoplasmic shuttling of the mRNA-binding protein HuR. *Cell Signal* 20:2165-2173.
- Du P, Kibbe WA, Lin SM (2008) lumi: a pipeline for processing Illumina microarray.

Bioinformatics 24:1547-1548.

Dugas JC, Notterpek L (2011) MicroRNAs in oligodendrocyte and Schwann cell differentiation. *Dev Neurosci* 33:14-20.

Echave P, Machado-da-Silva G, Arkell RS, Duchen MR, Jacobson J, Mitter R, Lloyd AC (2009) Extracellular growth factors and mitogens cooperate to drive mitochondrial biogenesis. *J Cell Sci* 122:4516-4525.

Feltri ML, Suter U, Relvas JB (2008) The function of RhoGTPases in axon ensheathment and myelination. *Glia* 56:1508-1517.

Fragoso G, Robertson J, Athlan E, Tam E, Almazan G, Mushynski WE (2003) Inhibition of p38 mitogen-activated protein kinase interferes with cell shape changes and gene expression associated with Schwann cell myelination. *Exp Neurol* 183:34-46.

Gomez-Sanchez JA, Lopez de Armentia M, Lujan R, Kessaris N, Richardson WD, Cabedo H (2009) Sustained axon-glia signaling induces Schwann cell hyperproliferation, Remak bundle myelination, and tumorigenesis. *J Neurosci* 29:11304-11315.

Gray LC, Hughes TR, van den Berg CW (2010) Binding of human antigen R (HuR) to an AU-rich element (ARE) in the 3'untranslated region (3'UTR) reduces the expression of decay accelerating factor (DAF). *Mol Immunol* 47:2545-2551.

Guo X, Wu Y, Hartley RS (2009) MicroRNA-125a represses cell growth by targeting HuR in breast cancer. *RNA Biol* 6:575-583.

Hieronymus H, Silver PA (2003) Genome-wide analysis of RNA-protein interactions illustrates specificity of the mRNA export machinery. *Nat Genet* 33:155-161.

Hinman MN, Lou H (2008) Diverse molecular functions of Hu proteins. *Cell Mol Life Sci* 65:3168-3181.

Houzelstein D, Bullock SL, Lynch DE, Grigorieva EF, Wilson VA, Beddington RS (2002)

- Growth and early postimplantation defects in mice deficient for the bromodomain-containing protein Brd4. *Mol Cell Biol* 22:3794-3802.
- Jacob C, Christen CN, Pereira JA, Somandin C, Baggiolini A, Lotscher P, Ozcelik M, Tricaud N, Meijer D, Yamaguchi T, Matthias P, Suter U (2011) HDAC1 and HDAC2 control the transcriptional program of myelination and the survival of Schwann cells. *Nat Neurosci* 14:429-436.
- Jena N, Deng M, Sicinska E, Sicinski P, Daley GQ (2002) Critical role for cyclin D2 in BCR/ABL-induced proliferation of hematopoietic cells. *Cancer Res* 62:535-541.
- Jessen KR, Mirsky R (2005) The origin and development of glial cells in peripheral nerves. *Nat Rev Neurosci* 6:671-682.
- Jessen KR, Mirsky R (2008) Negative regulation of myelination: relevance for development, injury, and demyelinating disease. *Glia* 56:1552-1565.
- Jeyaraj SC, Singh M, Ayupova DA, Govindaraju S, Lee BS (2010) Transcriptional control of human antigen R by bone morphogenetic protein. *J Biol Chem* 285:4432-4440.
- Kang MJ, Ryu BK, Lee MG, Han J, Lee JH, Ha TK, Byun DS, Chae KS, Lee BH, Chun HS, Lee KY, Kim HJ, Chi SG (2008) NF-kappaB activates transcription of the RNA-binding factor HuR, via PI3K-AKT signaling, to promote gastric tumorigenesis. *Gastroenterology* 135:2030-2042, 2042 e2031-2033.
- Katsanou V, Milatos S, Yiakouvaki A, Sgantzis N, Kotsoni A, Alexiou M, Harokopos V, Aidinis V, Hemberger M, Kontoyiannis DL (2009) The RNA-binding protein Elavl1/HuR is essential for placental branching morphogenesis and embryonic development. *Mol Cell Biol* 29:2762-2776.
- Kazan H, Ray D, Chan ET, Hughes TR, Morris Q (2010) RNAcontext: a new method for learning the sequence and structure binding preferences of RNA-binding proteins.

- PLoS Comput Biol 6:e1000832.
- Keene JD (2007) RNA regulons: coordination of post-transcriptional events. *Nat Rev Genet* 8:533-543.
- Keene JD, Komisarow JM, Friedersdorf MB (2006) RIP-Chip: the isolation and identification of mRNAs, microRNAs and protein components of ribonucleoprotein complexes from cell extracts. *Nat Protoc* 1:302-307.
- Kim HA, Pomeroy SL, Whoriskey W, Pawlitzky I, Benowitz LI, Sicinski P, Stiles CD, Roberts TM (2000) A developmentally regulated switch directs regenerative growth of Schwann cells through cyclin D1. *Neuron* 26:405-416.
- Kumar S (2009) Caspase 2 in apoptosis, the DNA damage response and tumour suppression: enigma no more? *Nat Rev Cancer* 9:897-903.
- Lankat-Buttgereit B, Goke R (2009) The tumour suppressor Pcd4: recent advances in the elucidation of function and regulation. *Biol Cell* 101:309-317.
- Larsson C (2006) Protein kinase C and the regulation of the actin cytoskeleton. *Cell Signal* 18:276-284.
- Lebedeva S, Jens M, Theil K, Schwanhaussner B, Selbach M, Landthaler M, Rajewsky N (2011) Transcriptome-wide analysis of regulatory interactions of the RNA-binding protein HuR. *Mol Cell* 43:340-352.
- Lee H, Cha S, Lee MS, Cho GJ, Choi WS, Suk K (2003) Role of antiproliferative B cell translocation gene-1 as an apoptotic sensitizer in activation-induced cell death of brain microglia. *J Immunol* 171:5802-5811.
- Li S, Millward S, Roberts R (2002) In vitro selection of mRNA display libraries containing an unnatural amino acid. *J Am Chem Soc* 124:9972-9973.
- Liang CC, Park AY, Guan JL (2007) In vitro scratch assay: a convenient and inexpensive

- method for analysis of cell migration in vitro. *Nat Protoc* 2:329-333.
- Liao JH, Chen JS, Chai MQ, Zhao S, Song JG (2001) The involvement of p38 MAPK in transforming growth factor beta1-induced apoptosis in murine hepatocytes. *Cell Res* 11:89-94.
- Limpert AS, Carter BD (2010) Axonal neuregulin 1 type III activates NF-kappaB in Schwann cells during myelin formation. *J Biol Chem* 285:16614-16622.
- Lincoln J, Kist R, Scherer G, Yutzey KE (2007) Sox9 is required for precursor cell expansion and extracellular matrix organization during mouse heart valve development. *Dev Biol* 305:120-132.
- Lino MM, Atanasoski S, Kvajo M, Fayard B, Moreno E, Brenner HR, Suter U, Monard D (2007) Mice lacking protease nexin-1 show delayed structural and functional recovery after sciatic nerve crush. *J Neurosci* 27:3677-3685.
- Lyons DA, Pogoda HM, Voas MG, Woods IG, Diamond B, Nix R, Arana N, Jacobs J, Talbot WS (2005) *erbb3* and *erbb2* are essential for schwann cell migration and myelination in zebrafish. *Curr Biol* 15:513-524.
- Mansfield KD, Keene JD (2009) The ribonome: a dominant force in co-ordinating gene expression. *Biol Cell* 101:169-181.
- Maurel P, Salzer JL (2000) Axonal regulation of Schwann cell proliferation and survival and the initial events of myelination requires PI 3-kinase activity. *J Neurosci* 20:4635-4645.
- Mazan-Mamczarz K, Hagner PR, Dai B, Wood WH, Zhang Y, Becker KG, Liu Z, Gartenhaus RB (2008) Identification of transformation-related pathways in a breast epithelial cell model using a ribonomics approach. *Cancer Res* 68:7730-7735.
- Morrissey TK, Levi AD, Nuijens A, Sliwkowski MX, Bunge RP (1995) Axon-induced

- mitogenesis of human Schwann cells involves heregulin and p185erbB2. *Proc Natl Acad Sci U S A* 92:1431-1435.
- Mukherjee N, Corcoran DL, Nusbaum JD, Reid DW, Georgiev S, Hafner M, Ascano M, Jr., Tuschl T, Ohler U, Keene JD (2011) Integrative regulatory mapping indicates that the RNA-binding protein HuR couples pre-mRNA processing and mRNA stability. *Mol Cell* 43:327-339.
- Mukherjee N, Lager PJ, Friedersdorf MB, Thompson MA, Keene JD (2009) Coordinated posttranscriptional mRNA population dynamics during T-cell activation. *Mol Syst Biol* 5:288.
- Nickols JC, Valentine W, Kanwal S, Carter BD (2003) Activation of the transcription factor NF-kappaB in Schwann cells is required for peripheral myelin formation. *Nat Neurosci* 6:161-167.
- Nodari A, Zambroni D, Quattrini A, Court FA, D'Urso A, Recchia A, Tybulewicz VL, Wrabetz L, Feltri ML (2007) Beta1 integrin activates Rac1 in Schwann cells to generate radial lamellae during axonal sorting and myelination. *J Cell Biol* 177:1063-1075.
- Pankov R, Endo Y, Even-Ram S, Araki M, Clark K, Cukierman E, Matsumoto K, Yamada KM (2005) A Rac switch regulates random versus directionally persistent cell migration. *J Cell Biol* 170:793-802.
- Parkinson DB, Bhaskaran A, Arthur-Farraj P, Noon LA, Woodhoo A, Lloyd AC, Feltri ML, Wrabetz L, Behrens A, Mirsky R, Jessen KR (2008) c-Jun is a negative regulator of myelination. *J Cell Biol* 181:625-637.
- Parkinson DB, Bhaskaran A, Droggiti A, Dickinson S, D'Antonio M, Mirsky R, Jessen KR (2004) Krox-20 inhibits Jun-NH2-terminal kinase/c-Jun to control Schwann cell proliferation and death. *J Cell Biol* 164:385-394.

- Parkinson DB, Dong Z, Bunting H, Whitfield J, Meier C, Marie H, Mirsky R, Jessen KR (2001) Transforming growth factor beta (TGFbeta) mediates Schwann cell death in vitro and in vivo: examination of c-Jun activation, interactions with survival signals, and the relationship of TGFbeta-mediated death to Schwann cell differentiation. *J Neurosci* 21:8572-8585.
- Peart MJ, Smyth GK, van Laar RK, Bowtell DD, Richon VM, Marks PA, Holloway AJ, Johnstone RW (2005) Identification and functional significance of genes regulated by structurally different histone deacetylase inhibitors. *Proc Natl Acad Sci U S A* 102:3697-3702.
- Pullmann R, Jr., Kim HH, Abdelmohsen K, Lal A, Martindale JL, Yang X, Gorospe M (2007) Analysis of turnover and translation regulatory RNA-binding protein expression through binding to cognate mRNAs. *Mol Cell Biol* 27:6265-6278.
- Raphael AR, Lyons DA, Talbot WS (2011) ErbB signaling has a role in radial sorting independent of Schwann cell number. *Glia* 59:1047-1055.
- Riedl SJ, Salvesen GS (2007) The apoptosome: signalling platform of cell death. *Nat Rev Mol Cell Biol* 8:405-413.
- Rouschop KM, Claessen N, Pals ST, Weening JJ, Florquin S (2006) CD44 disruption prevents degeneration of the capillary network in obstructive nephropathy via reduction of TGF-beta1-induced apoptosis. *J Am Soc Nephrol* 17:746-753.
- Salim C, Boxberg YV, Alterio J, Fereol S, Nothias F (2009) The giant protein AHNAK involved in morphogenesis and laminin substrate adhesion of myelinating Schwann cells. *Glia* 57:535-549.
- Shoshan-Barmatz V, De Pinto V, Zweckstetter M, Raviv Z, Keinan N, Arbel N (2010) VDAC, a multi-functional mitochondrial protein regulating cell life and death. *Mol*

- Aspects Med 31:227-285.
- Smyth G (2005) Limma: linear models for microarray data. In *Bioinformatics and computational biology solutions using R and bioconductor*:397-420.
- Stewart HJ, Morgan L, Jessen KR, Mirsky R (1993) Changes in DNA synthesis rate in the Schwann cell lineage in vivo are correlated with the precursor--Schwann cell transition and myelination. *Eur J Neurosci* 5:1136-1144.
- Tikoo R, Zanazzi G, Shiffman D, Salzer J, Chao MV (2000) Cell cycle control of Schwann cell proliferation: role of cyclin-dependent kinase-2. *J Neurosci* 20:4627-4634.
- Tomomura M, Fernandez-Gonzales A, Yano R, Yuzaki M (2001) Characterization of the apoptosis-associated tyrosine kinase (AATYK) expressed in the CNS. *Oncogene* 20:1022-1032.
- Topilko P, Schneider-Maunoury S, Levi G, Baron-Van Evercooren A, Chennoufi AB, Seitanidou T, Babinet C, Charnay P (1994) Krox-20 controls myelination in the peripheral nervous system. *Nature* 371:796-799.
- Vazquez-Chantada M, Ariz U, Varela-Rey M, Embade N, Martinez-Lopez N, Fernandez-Ramos D, Gomez-Santos L, Lamas S, Lu SC, Martinez-Chantar ML, Mato JM (2009) Evidence for LKB1/AMP-activated protein kinase/ endothelial nitric oxide synthase cascade regulated by hepatocyte growth factor, S-adenosylmethionine, and nitric oxide in hepatocyte proliferation. *Hepatology* 49:608-617.
- Verheijen MH, Chrast R, Burrola P, Lemke G (2003) Local regulation of fat metabolism in peripheral nerves. *Genes Dev* 17:2450-2464.
- Ward AC, Smith L, de Koning JP, van Aesch Y, Touw IP (1999) Multiple signals mediate proliferation, differentiation, and survival from the granulocyte colony-stimulating factor receptor in myeloid 32D cells. *J Biol Chem* 274:14956-14962.

- Witke W (2004) The role of profilin complexes in cell motility and other cellular processes. *Trends Cell Biol* 14:461-469.
- Woodhoo A, Alonso MB, Droggiti A, Turmaine M, D'Antonio M, Parkinson DB, Wilton DK, Al-Shawi R, Simons P, Shen J, Guillemot F, Radtke F, Meijer D, Feltri ML, Wrabetz L, Mirsky R, Jessen KR (2009) Notch controls embryonic Schwann cell differentiation, postnatal myelination and adult plasticity. *Nat Neurosci* 12:839-847.
- Woodhoo A, Sommer L (2008) Development of the Schwann cell lineage: from the neural crest to the myelinated nerve. *Glia* 56:1481-1490.
- Xiao L, Rao JN, Zou T, Liu L, Marasa BS, Chen J, Turner DJ, Zhou H, Gorospe M, Wang JY (2007) Polyamines regulate the stability of activating transcription factor-2 mRNA through RNA-binding protein HuR in intestinal epithelial cells. *Mol Biol Cell* 18:4579-4590.
- Xie S, Sukkar MB, Issa R, Khorasani NM, Chung KF (2007) Mechanisms of induction of airway smooth muscle hyperplasia by transforming growth factor-beta. *Am J Physiol Lung Cell Mol Physiol* 293:L245-253.
- Yang DP, Zhang DP, Mak KS, Bonder DE, Pomeroy SL, Kim HA (2008) Schwann cell proliferation during Wallerian degeneration is not necessary for regeneration and remyelination of the peripheral nerves: axon-dependent removal of newly generated Schwann cells by apoptosis. *Mol Cell Neurosci* 38:80-88.
- Yano K, Bauchat JR, Liimatta MB, Clemmons DR, Duan C (1999) Down-regulation of protein kinase C inhibits insulin-like growth factor I-induced vascular smooth muscle cell proliferation, migration, and gene expression. *Endocrinology* 140:4622-4632.
- Yi J, Chang N, Liu X, Guo G, Xue L, Tong T, Gorospe M, Wang W (2010) Reduced nuclear export of HuR mRNA by HuR is linked to the loss of HuR in replicative senescence.

Nucleic Acids Res 38:1547-1558.

Yu WM, Yu H, Chen ZL, Strickland S (2009) Disruption of laminin in the peripheral nervous system impedes nonmyelinating Schwann cell development and impairs nociceptive sensory function. *Glia* 57:850-859.

FIGURE LEGENDS

Figure 1: HuR is differentially expressed in postnatal sciatic nerves

HuR expression is significantly reduced in P10 nerves, compared to NB and P5, as shown by (a) qPCR, (b) Western blotting of total protein extracts and (c) cytosolic and nuclear protein fractions. (d) IHC showing HuR expression (*red*) in Schwann cells from P5 teased sciatic nerves (arrows). TuJ1 labels axons (*green*) and DAPI labels nuclei (*blue*). (b,c) Gapdh/ β -actin: loading control. (c) Gapdh: cytoplasmic marker; Histone H3: nuclear marker. Data: mean \pm s.e.m; * $p < 0.01$.

Figure 2: RIP-ChIP identifies several HuR targets *in vivo* in NB and P5 nerves

(a) Heatmap showing expression of the top transcripts most significantly bound to HuR compared to control IgG in NB nerves (*upper panel*) and P5 nerves (*bottom panel*) in 4 different replicates (1-4). (b) Heatmap showing relative enrichment of top 50 mRNA targets of HuR, compared to control IgG (HuR IP/ IgG IP, Column 1) and input mRNA (HuR IP/ Input, Column 2). The colour scale indicates the degree of enrichment (green-red ratio scale). (c) Venn diagram showing the overlap of HuR-bound transcripts with a fold change ≥ 1.5 in lysates isolated from NB and P5 nerves. (d) Enriched Gene Ontology (GO) classification of the genes identified by the RIP-chip analyses in NB (*blue* histograms) and P5 nerves (*red* histograms).

Figure 3: HuR mediates laminin-induced HuR motility and morphogenesis

(a) Cell scratch assay showing that migration on laminin-coated coverslips is significantly reduced in sh HuR-infected cells (***) compared to sh Control-infected cells (*). (b) Graphs showing the closure of the gap distance with time after culture

on laminin-coated coverslips. (c) Talin ICC (*red*) showing morphological differences between sh HuR-infected and sh Control-infected cells plated onto laminin. (d) *HuR*-silenced cells have a smaller surface area and fewer lamellipodia on laminin substrate, but not on PDL. (e) *HuR*-silenced cells have shorter axial lamellipodia and fewer radial lamellipodia than sh Control-infected cells on laminin. (f) qPCR showing expression of different transcripts after culture on laminin with time, expressed as fold change relative to cells replated onto PDL dishes. (g) RIP-qPCR analysis shows significant enrichment of several motility/morphology-associated genes bound to HuR in cells plated onto laminin compared to cells plated onto PDL. (h) *HuR* silencing leads to a significant reduction in expression of these genes.

Figure 4: Laminin induces nucleo-cytoplasmic translocation of HuR

(a) Western blot showing nucleo-cytoplasmic translocation of HuR after replating of Schwann cells onto laminin. (b, c) Western blot showing that treatment with SB203580 (to block p38 phosphorylation) (b) prevents the nucleo-cytoplasmic translocation of HuR after 4h culture onto laminin and (c) reduces the migration rate on laminin. (a,b) β -actin: loading control; (a) Gapdh: cytoplasmic marker; Histone H3: nuclear marker. Cyto: cytoplasmic fractions; Nucl: Nuclear fractions. Data: mean \pm s.e.m; * $p < 0.01$

Figure 5: HuR mediates NRG1 and TGF β -induced proliferation

(a, b) *HuR* silencing significantly reduces (a) NRG1- and (b) TGF β -induced proliferation compared to sh Control-infected cells as determined by BrdU incorporation (BrdU⁺ cells: *red*; Dapi⁺ Nuclei: *blue*). (c) qPCR showing expression of

different transcripts after NRG1 or TGF β treatment with time, expressed as fold change relative to untreated cells. **(d)** RIP-qPCR analysis shows significant enrichment of proliferation-associated genes bound to HuR in NRG1- and TGF β -treated cells compared to cells cultured in MM. **(e, f)** *HuR* silencing leads to a significant reduction in expression of proliferation-associated genes after **(e)** NRG1 and **(f)** TGF β treatment. Data: mean \pm s.e.m; * p <0.01

Figure 6: NRG1 and TGF β induce nucleo-cytoplasmic translocation of HuR

(a) Western blot showing nucleo-cytoplasmic translocation of HuR after NRG1 and TGF β treatment. **(b)** Treatment with UO126 (to block ERK 1/2 phosphorylation) or LY-294002 (to block AKT phosphorylation) prevents NRG1-induced nucleo-cytoplasmic translocation of HuR (*left panel*) and proliferation (*right panel*). **(c)** Treatment with UO126 or SB203580 prevents TGF β -induced nucleo-cytoplasmic translocation of HuR (*left panel*) and proliferation (*right panel*). **(a-c)** β -actin; loading control. **(a)** Gapdh: cytoplasmic marker; Histone H3: nuclear marker. Cyto: cytoplasmic fractions; Nucl: Nuclear fractions. Data: mean \pm s.e.m; * p <0.01

Figure 7: HuR mediates TGF β -induced apoptosis

(a, b) *HuR* silencing leads to a significant reduction in TGF β -apoptosis as seen by **(a)** number of surviving cells identified by nuclear condensation viewed by DAPI (*blue*) and number of apoptotic cells viewed by Tunel labelling (*green*), and **(b)** Western blot of PARP cleavage and active caspase-3, 48h after treatment. **(c)** qPCR showing expression of different transcripts after TGF β treatment with time,

expressed as fold change relative to untreated cells. (d) RIP-qPCR analysis shows significant enrichment of apoptosis-associated genes bound to HuR in TGF β -treated cells compared to cells cultured in SM. (e) *HuR* silencing leads to a significant reduction in expression of these genes. (f) Western blot showing nucleo-cytoplasmic translocation of HuR after TGF β treatment. (g, h) Treatment with SB203580, but not with UO126, prevents TGF β -induced (g) nucleo-cytoplasmic translocation of HuR and (h) apoptosis. (f,g) β -actin; loading control. (f) Gapdh: cytoplasmic marker; Histone H3: nuclear marker. Cyto: cytoplasmic fractions; Nucl: Nuclear fractions. Data: mean \pm s.e.m; *p<0.01

Figure 8: HuR is a negative regulator of myelination

(a) RIP-qPCR analysis shows binding of HuR to *Pmp22* mRNA both in NB and P5 nerves. (b) Schematic of *Pmp22* mRNA depicting the 5' UTR, Coding Region and 3'UTR. In silico analysis revealed several computationally predicted HuR motifs (arrowheads), and biotinylated transcripts spanning different mRNA regions (A-E) were incubated with P5 sciatic nerve lysates and the interaction assessed by biotin pull-down assays followed by Western blot analysis. HuR only formed complexes with a specific region of the 3' UTR, but not with the 5' UTR or coding region. No interaction was seen with a control biotinylated RNA corresponding to the 3'UTR of *GAPDH* mRNA, which is not a target of HuR (data not shown). (c) RIP-qPCR analysis shows binding of HuR to several myelination-related genes in postnatal nerves. (d) Western blot showing an increased expression of several myelination genes after *HuR* silencing under basal (MM) and myelinogenic conditions (dibutryl cAMP treatment). (e, f) qPCR showing an increased expression of myelination-

related genes after HuR silencing (e) in MM, and (f) after cAMP treatment. (g) qPCR showing the half-life of myelination-related genes in control and *HuR*-silenced cAMP-treated cells.

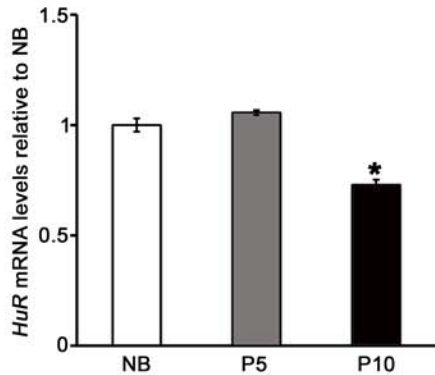
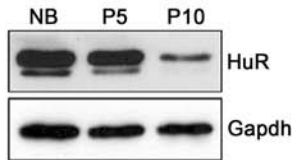
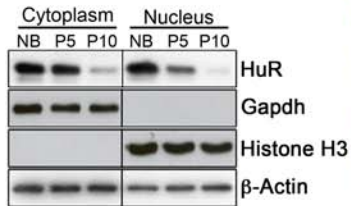
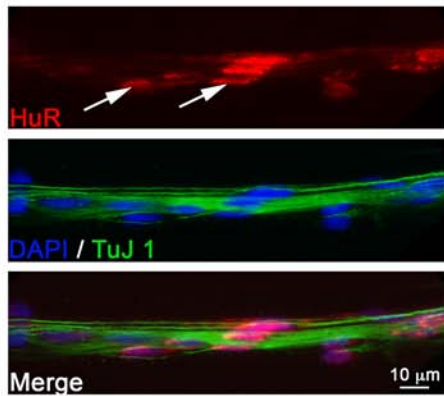
Figure 9: HuR regulates myelination in DRG co-cultures

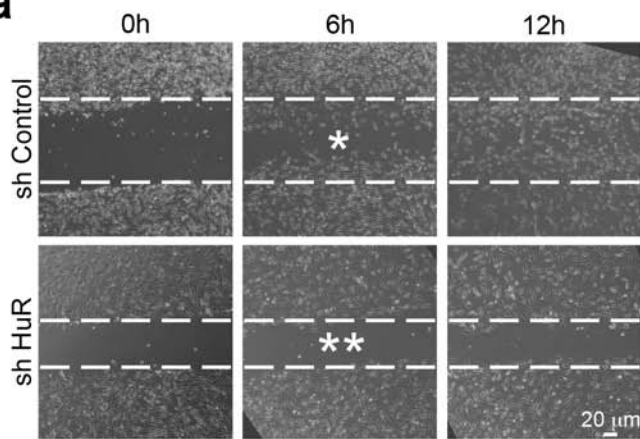
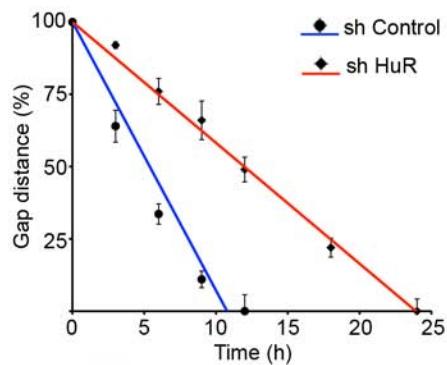
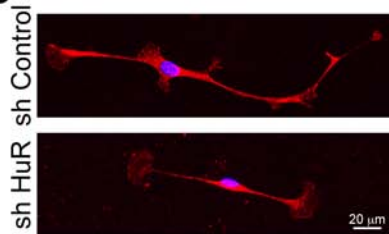
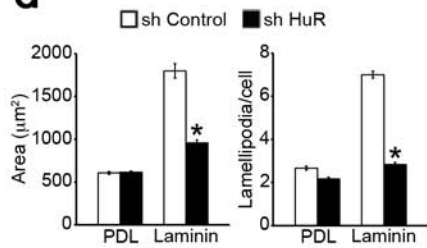
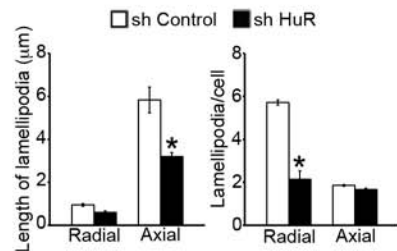
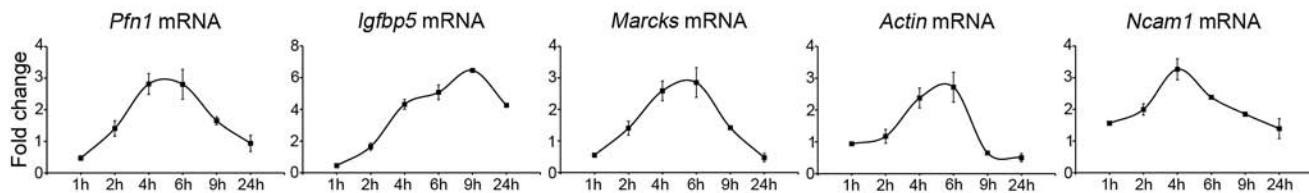
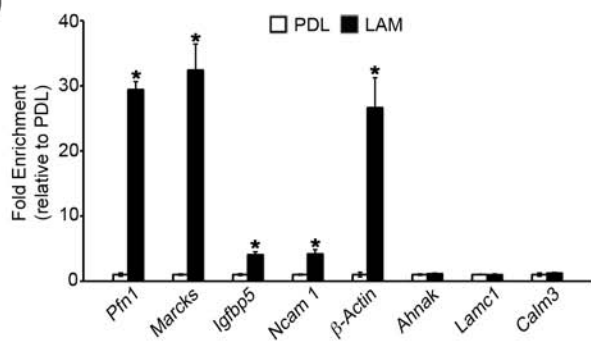
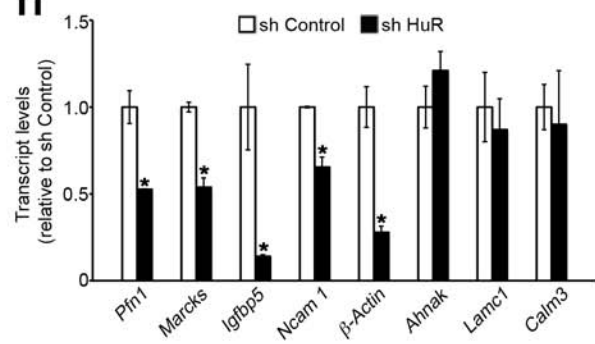
(a, b) *HuR* silencing increases myelination in Schwann cell-DRG co-cultures, as seen by (a) number of MBP⁺ myelin segments (*red*), and (b) qPCR analysis of myelination-related genes. (c, d) Enforced *HuR* expression induced a small but significant decrease in myelination in Schwann cell-DRG co-cultures, as seen by (c) number of MBP⁺ myelin segments (*red*), and (d) qPCR analysis of myelination-related genes. Gapdh; loading control. Data: mean ± s.e.m; *p<0.01

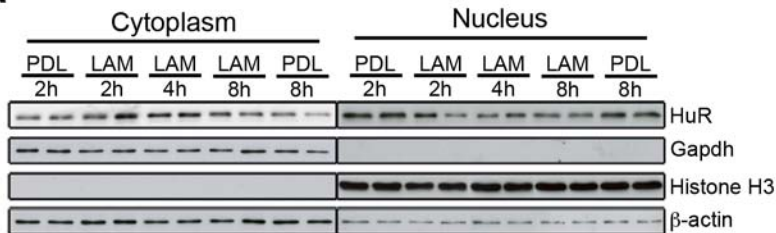
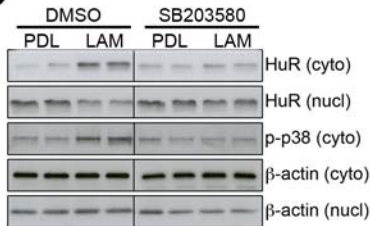
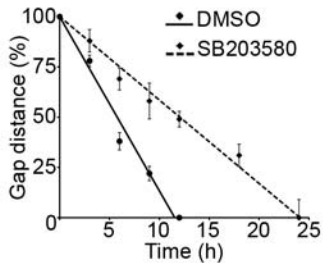
Figure 10: HuR expression is controlled by p65 and Smad2/3-induced transcription

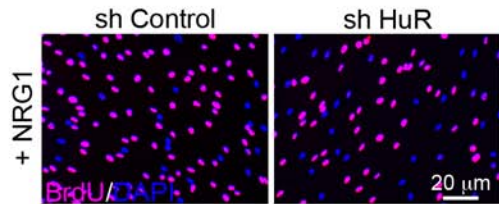
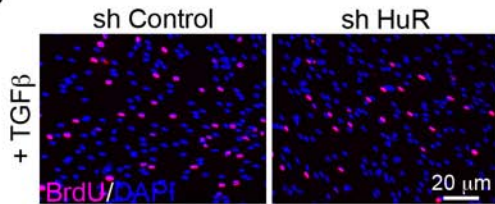
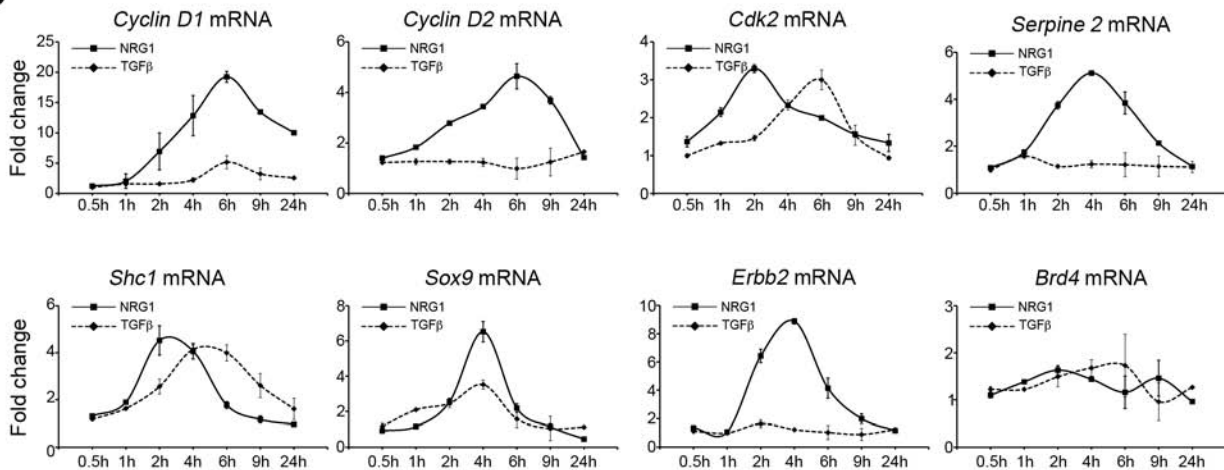
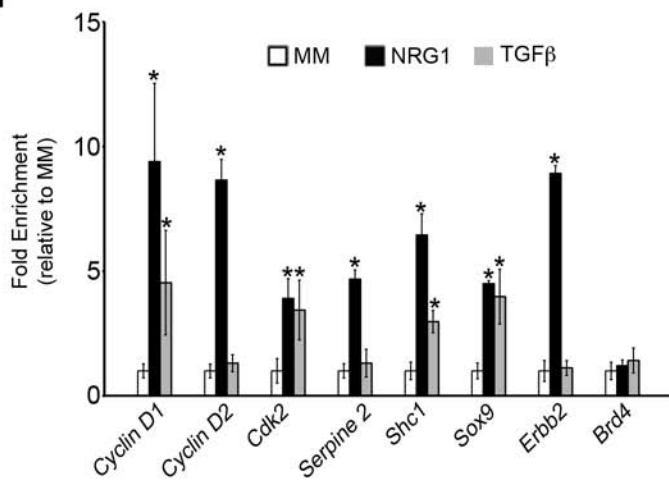
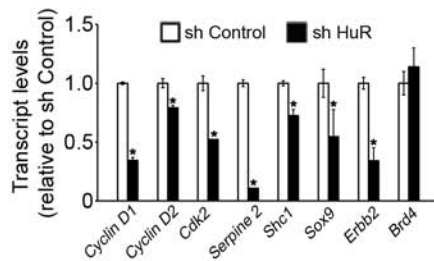
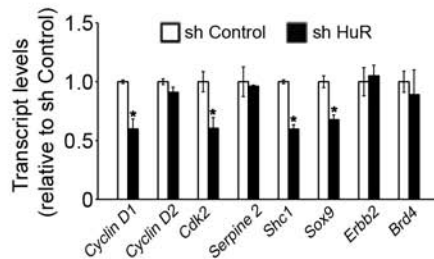
(a, b) Schematic diagram of the promoter region of *HuR* showing (a) NFκB consensus binding sites (green ovals) and regions analysed (A1 and A2) and (b) SMAD 2/3 consensus binding sites (yellow ovals) and regions analysed (B1 and B2). ChIP analysis shows a decreased binding of p65 and SMAD 2/3 to the regions analysed, in P10 nerves compared to NB and P5 nerves. (c) Western blot showing reduced p65 and SMAD 2/3 expression in nuclear fractions of P10 nerves compared to NB and P5 nerves. (d-f) NRG1 increases *HuR* transcription through NFκB activation. (d) Treatment with NRG1 increases *HuR* mRNA (*upper panel*) and *HuR* protein levels (*bottom panel*), as seen by qPCR and Western blotting respectively. (e) ChIP analysis shows that p65 is recruited to the *HuR* promoter regions (indicated

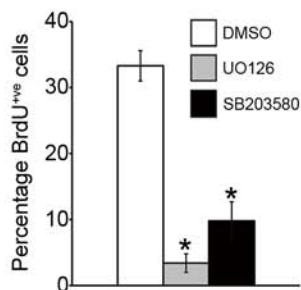
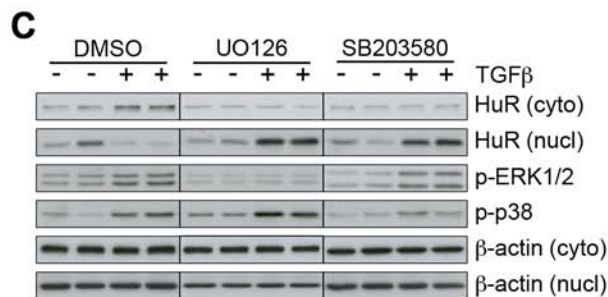
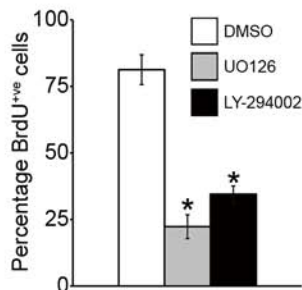
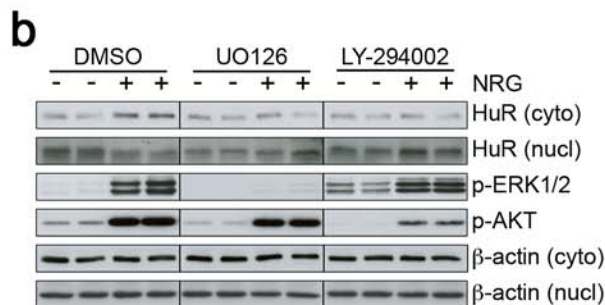
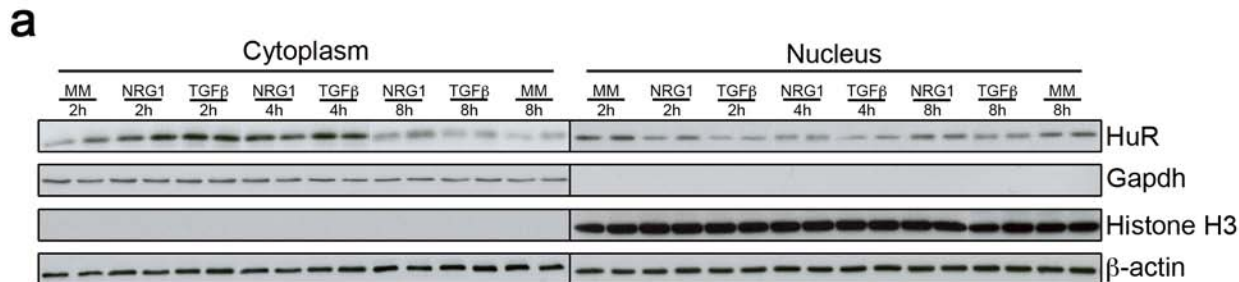
in **a**) after treatment with NRG1 for 1 hr, but not in cells cultured in MM, or with NRG1 for 12 hrs. **(f)** Western blot showing that treatment with the NF κ B inhibitor BAY11-7082, which prevents the nuclear translocation of p65, inhibits the NRG1-induced increase in HuR levels. **(g-i)** TGF β increases *HuR* transcription through SMAD2/3 activation. **(g)** Treatment with TGF β increases *HuR* mRNA (*upper panel*) and HuR protein levels (*bottom panel*), as seen by qPCR and Western blotting respectively. **(h)** ChIP analysis shows that SMAD2/3 is recruited to the *HuR* promoter regions (indicated in **b**) after treatment with TGF β for 1 hr, but not in cells cultured in MM, or with TGF β for 12 hrs. **(i)** Western blot showing that adenoviral infection of cells with SMAD7 adenovirus (Ad-SMAD7), which prevents the nuclear translocation of SMAD2/3, inhibits the TGF β -induced increase in HuR levels. **(j)** Combined treatment of NRG1 and TGF β of Schwann cells plated onto laminin did not lead to an enhanced upregulation of HuR, induced by the two growth factors alone, as seen by qPCR (*upper panel*) and Western blot (*bottom panel*), 2h after treatment. **(k, l)** Western blots showing that adenoviral infection of cells with Egr2 adenovirus (Ad-Egr2), **(k)** decreases HuR levels after 48 hrs, **(l)** an effect reduced with treatment with the proteasome inhibitor MG132. β -actin/Gapdh; loading control. Nuc: Nuclear fractions. Data: mean \pm s.e.m; * $p < 0.01$

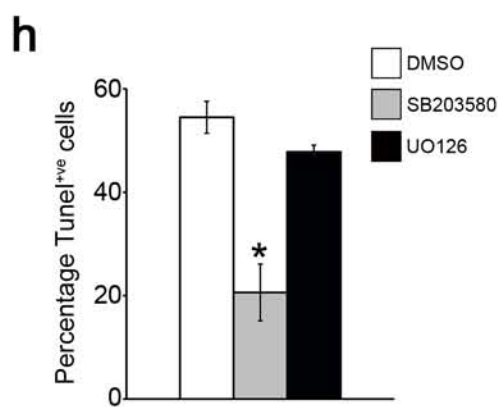
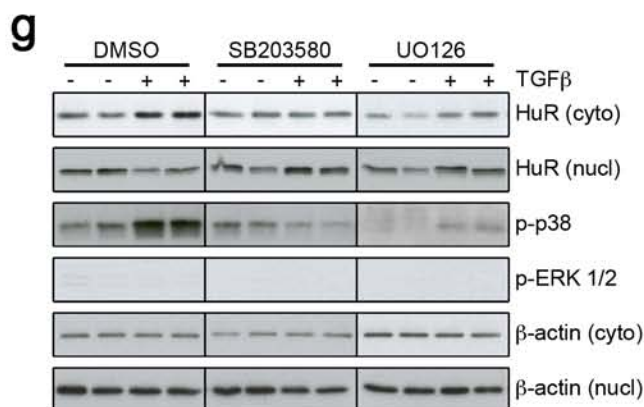
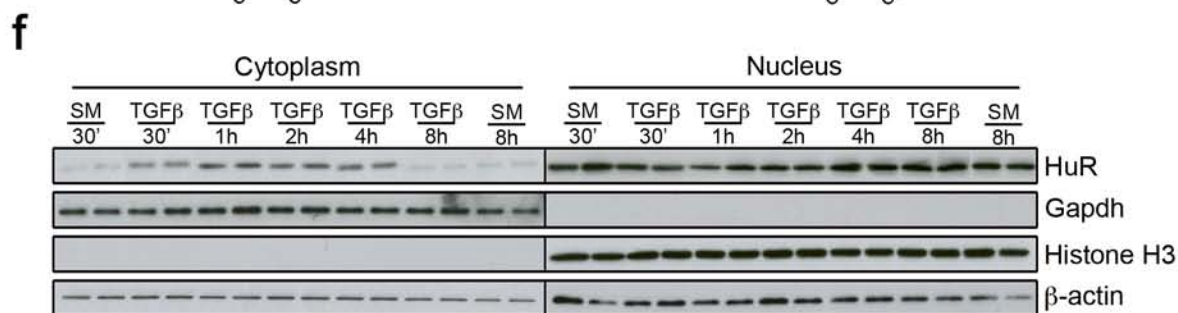
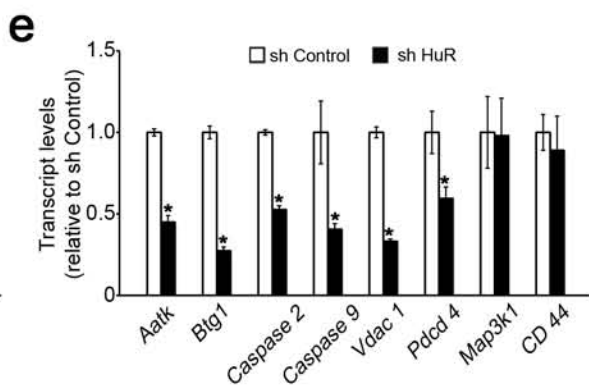
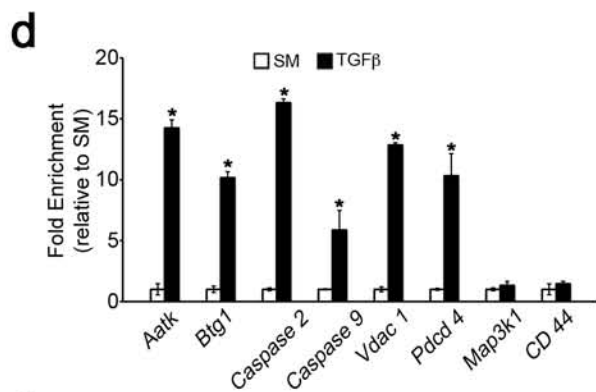
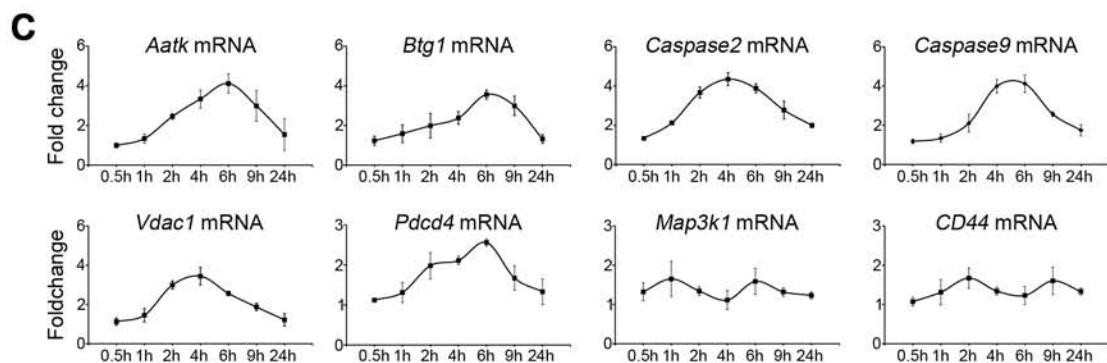
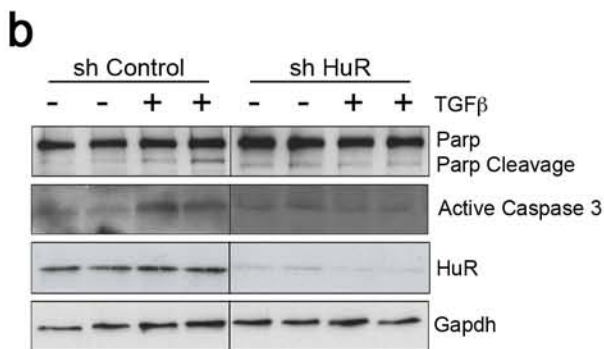
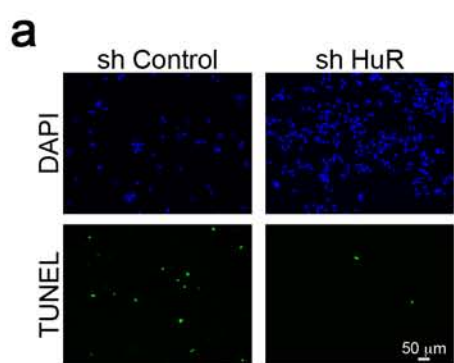
a**b****c****d**

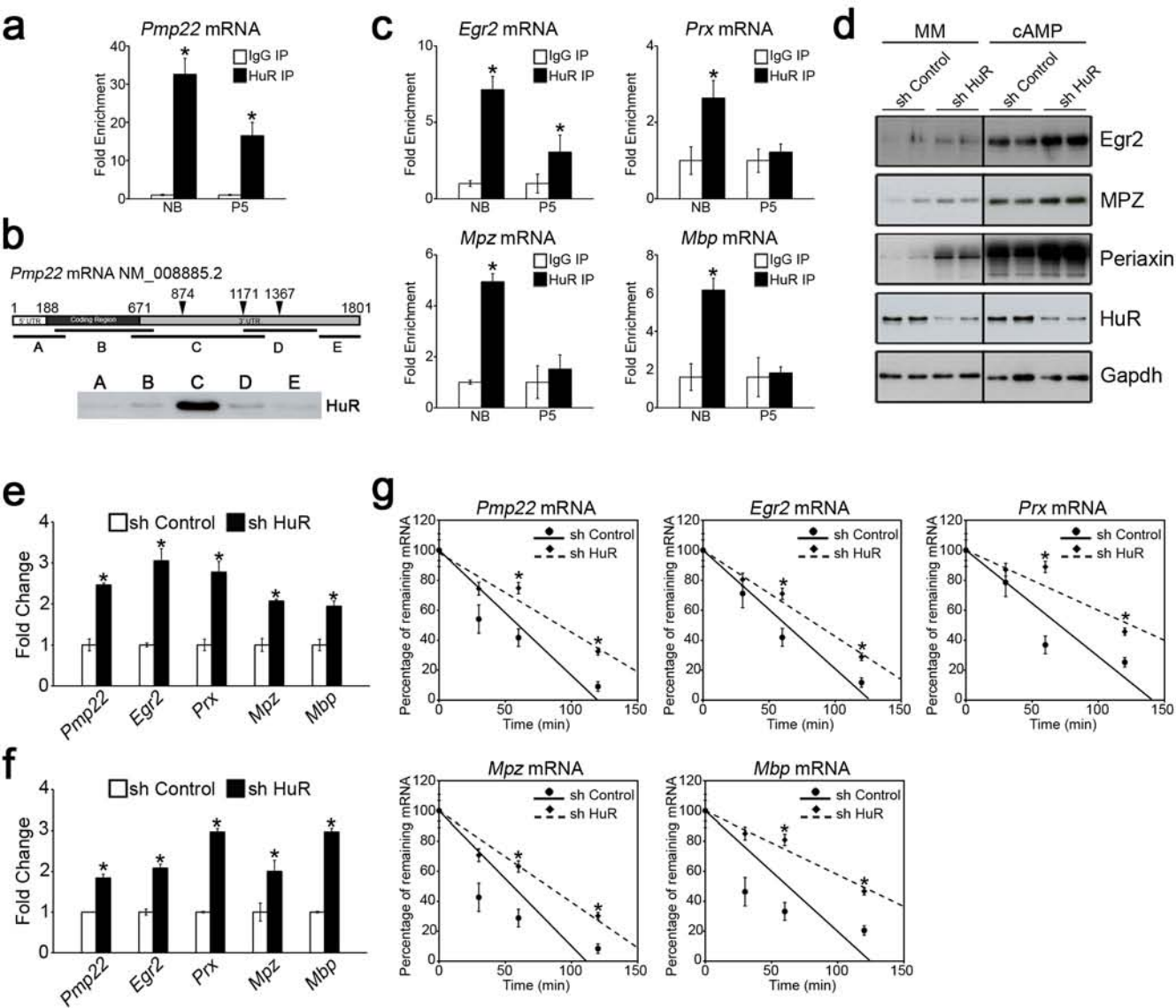
a**b****c****d****e****f****g****h**

a**b****c**

a**b****c****d****e****f**

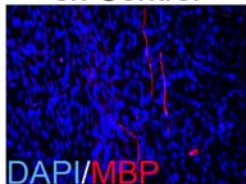




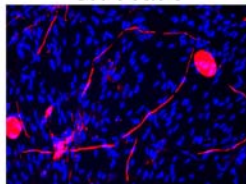


a

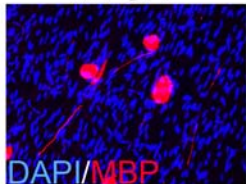
sh Control



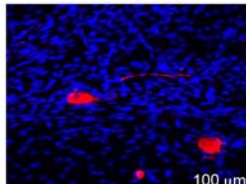
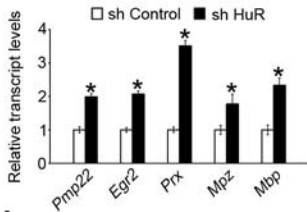
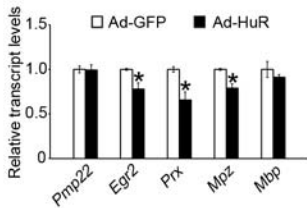
sh HuR

**c**

Ad-GFP



Ad-HuR

**b****d**

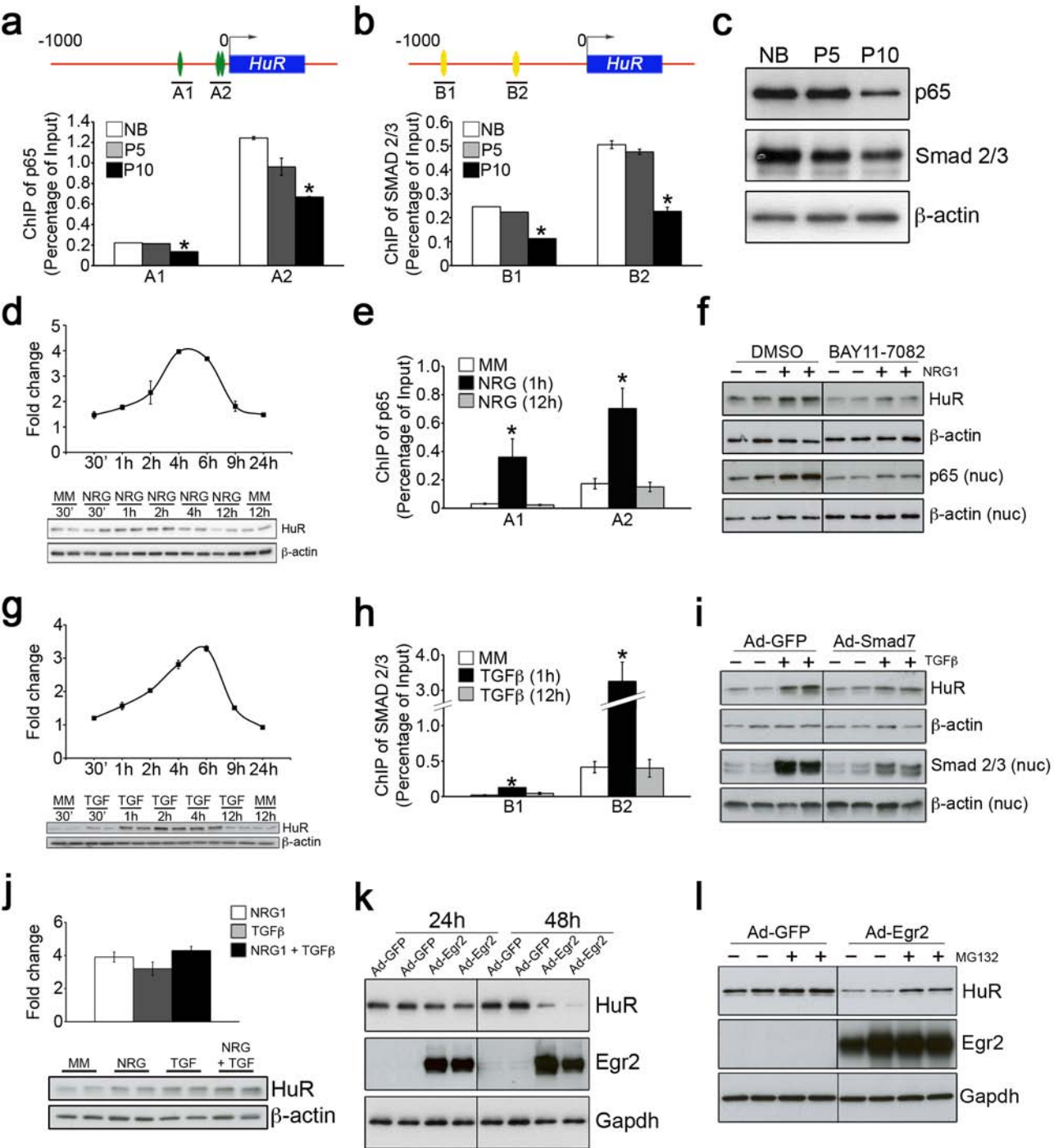


Table 1: Validation of RIP-ChIP by RIP-qPCR

| | Gene Symbol | Gene Name | NB | | P5 | |
|------------------------|-----------------|---|-------|-------|---------------------|--------------------|
| | | | Array | qPCR | Array | qPCR |
| Proliferation | <i>Ccnd1</i> | cyclin D1 | 5.54* | 5.17* | 1.32 ^{ns} | 1.12 ^{ns} |
| | <i>Ccnd2</i> | cyclin D2 | 1.56* | 2.31* | 1.41 ^{ns} | 1.19 ^{ns} |
| | <i>Cdk2</i> | cyclin-dependent kinase 2 | 2.55* | 3.35* | 1.29 ^{ns} | 1.63 ^{ns} |
| | <i>Serpine2</i> | serine (or cysteine) peptidase inhibitor, clade E, member 2 | 1.78* | 3.74* | -1.04 ^{ns} | 1.61 ^{ns} |
| | <i>Brd4</i> | bromodomain containing 4 | 2.13* | 3.73* | 1.29 ^{ns} | 1.12 ^{ns} |
| | <i>ErbB2</i> | v-erb-b2 erythroblastic leukemia viral oncogene homolog 2 | 1.76* | 5.17* | 1.00 ^{ns} | 1.09 ^{ns} |
| | <i>Sox9</i> | SRY-box containing gene 9 | 3.38* | 7.86* | 1.70* | 3.93* |
| | <i>Shc1</i> | src homology 2 domain-containing transforming protein C1 | 3.19* | 6.52* | 1.35 ^{ns} | 1.09 ^{ns} |
| Cell Morphology | <i>Actb</i> | actin, beta | 59.1* | 63.9* | 26.3* | 29.5* |
| | <i>Ncam1</i> | neural cell adhesion molecule 1 | 2.34* | 4.65* | 1.38 ^{ns} | 1.06 ^{ns} |
| | <i>Pfn1</i> | profilin 1 | 3.98* | 4.65* | 5.56* | 5.08* |
| | <i>Ahnak</i> | AHNAK nucleoprotein (desmoyokin) | 16.5* | 12.7* | 6.79* | 6.89* |
| | <i>Lamc1</i> | laminin, gamma 1 | 2.32* | 4.45* | 1.06 ^{ns} | 1.35 ^{ns} |
| | <i>Calm3</i> | calmodulin 3 | 6.62* | 16.1* | 2.66* | 7.18* |
| | <i>Igfbp5</i> | insulin-like growth factor binding protein 5 | 4.29* | 3.86* | 1.69 ^{ns} | 1.51 ^{ns} |
| | <i>Marcks</i> | myristoylated alanine-rich protein kinase C substrate | 4.57* | 9.83* | 1.15 ^{ns} | 1.60 ^{ns} |
| Apoptosis | <i>Casp2</i> | caspase 2 | 1.99* | 5.11* | 1.14 ^{ns} | 1.87 ^{ns} |
| | <i>Casp9</i> | caspase 9 | 1.89* | 3.68* | 1.32 ^{ns} | 1.68 ^{ns} |
| | <i>Aatk</i> | apoptosis-associated tyrosine kinase | 7.08* | 12.6* | 2.74* | 5.20* |
| | <i>Btg1</i> | B-cell translocation gene 1 | 2.82* | 4.71* | 1.13 ^{ns} | 1.58 ^{ns} |
| | <i>Map3k1</i> | mitogen-activated protein kinase kinase kinase 1 | 1.7* | 4.51* | 1.12 ^{ns} | 1.14 ^{ns} |
| | <i>Cd44</i> | CD44 antigen | 1.99* | 6.24* | 1.47 ^{ns} | 5.01* |
| | <i>Pdcd4</i> | programmed cell death 4 | 2.57* | 8.60* | 2.11* | 7.48* |
| | <i>Vdac1</i> | voltage-dependent anion channel 1 | 3.09* | 6.14* | 1.82 ^{ns} | 3.63* |

